ELSEVIER

Physica D 167 (2002) 218–247

PHYSICA D

www.elsevier.com/locate/physd

A Galërkin approach to electronic near-degeneracies in molecular systems

Mason A. Porter [a,*], Richard L. Liboff [a,b,c]

[a] *Center for Applied Mathematics, Cornell University, 657 Frank T. Rhodes Hall, Ithaca, NY 14853, USA*
[b] *Department of Electrical and Computer Engineering, Cornell University, Phillips Hall, Ithaca, NY, USA*
[c] *Department of Applied and Engineering Physics, Cornell University, Clark Hall, Ithaca, NY, USA*

Received 18 May 2001; received in revised form 25 January 2002; accepted 26 March 2002
Communicated by E. Bodenschatz

Abstract

We consider superposition states of various numbers of eigenstates in order to study vibrating quantum billiards semiquantally. We discuss the relationship between Galërkin methods, inertial manifolds, and partial differential equations such as nonlinear Schrödinger equations and Schrödinger equations with time-dependent boundary conditions. We then use a Galërkin approach to study vibrating quantum billiards. We consider one-term, two-term, three-term, d-term, and infinite-term superposition states. The number of terms under consideration corresponds to the level of electronic near-degeneracy in the system of interest. We derive a generalized Bloch transformation that is valid for any finite-term superposition and numerically simulate three-state superpositions of the radially vibrating spherical quantum billiard with null angular-momentum eigenstates. We discuss the physical interpretation of our Galërkin approach and thereby justify its use for vibrating quantum billiards. For example, d-term superposition states of one degree-of-vibration quantum billiards may be used to study nonadiabatic behavior in polyatomic molecules with one excited nuclear mode and a d-fold electronic near-degeneracy. Finally, we apply geometric methods to analyze the symmetries of vibrating quantum billiards.

PACS: 05.45.Mt; 05.45.Pq; 05.45.-a; 51.50.Gh; 31.15.Gy; 02.70.Dh

Keywords: Quantum chaos; Nonlinear dynamics; Semiclassical methods; Nonadiabatic couplings; Galërkin methods

1. Introduction

Quantum billiards have been studied extensively in recent years [11,13,20,21]. They are important tools in the study of quantum chaos. When their boundaries are time-dependent, they are also useful for probing *semiquantum chaos* [35], the primary concern of the present paper. This type of quantum chaos, whose phenomenology we discuss in Appendix A, pertains to chaos in semiquantum systems derived via a Born–Oppenheimer scheme [4,7–9,35]. In conservative situations, such systems may be expressed as "effective classical Hamiltonians" and analyzed using techniques from Hamiltonian dynamics [22,29,32,35,46,50].

* Corresponding author. Tel.: +1-607-255-3399; fax: +1-607-255-9860.
E-mail address: mason@cam.cornell.edu (M.A. Porter).

0167-2789/02/$ – see front matter
PII: S0167-2789(02)00449-9

Vibrating quantum billiards are semiquantum models for nonadiabatic coupling in polyatomic molecules [8,28, 38–40]. They may also be used as mathematical abstractions in the description of Jahn–Teller distortions [6,30,35, 46,50], nanomechanical vibrations [34] and solvated electrons [43,44]. Hence, the study of semiquantum chaos in quantum billiards with time-dependent boundaries is important both because it expands the mathematical theory of dynamical systems and because it can be applied to problems in atomic, molecular, and mesoscopic physics.

Blümel and Esser [8] found semiquantum chaos in the one-dimensional vibrating quantum billiard. In previous works [28,39], we extended these results to spherical quantum billiards with time-dependent surfaces and derived necessary conditions for vibrating quantum billiards with one "degree-of-vibration" (dov) to exhibit chaotic behavior [40]. The dov constitute the classical degrees-of-freedom (dof) in a vibrating quantum billiard and refer to the number of distance dimensions of the boundary that vary in time. Bifurcations of one dov quantum billiards have been analyzed [36], and we have recently performed some analysis of two dov quantum billiards [38].

Quantum systems with time-dependent potentials have been the subject of considerable attention in the quantum chaos literature. Such systems include, for example, Anderson transitions [10,12], Landau level mixing [42], the two-particle Harper problem [3], and amplitude-modulated pendula [33]. There are two important differences between these descriptions and the "vibrating quantum billiards" that interest us. First, we use a semiquantum description in order to examine systems with dof that evolve on multiple timescales. Studies like those cited above are concerned with the quantum signatures of classical chaos rather than with semiquantum chaos. We seek to connect the study of nonadiabatic phenomena (such as Jahn–Teller effects), which is of considerable interest in the molecular physics literature, to abstract mathematical models such as vibrating quantum billiards [6,7,30,35,46,50]. This abstraction leads to a second important distinction. In contrast to the works cited above, the time-dependence in the vibrating quantum billiards we discuss has not been specified a priori. Instead, it must be determined in the process of solving a boundary value problem (rather than in advance of attempting such a solution). The problem under consideration is thus said to have a *free boundary* [18].

With this perspective, one may use vibrating quantum billiards to study nonadiabatic transitions in molecular systems [32,35]. In particular, we are concerned with Jahn–Teller-like distortions in polyatomic molecules [6,24,30]. Associated with nonadiabatic behavior are d-fold near-degeneracies in the adiabatic sheets describing the eigenenergies of a molecule's electronic subsystem [7,46,50]. To analyze such near-degeneracies, one may study d-mode Galërkin projections (i.e., d-term superposition states) of vibrating quantum billiards.

Our previous work on quantum billiards with time-dependent boundaries concentrated primarily on two-term superposition states [8,9,28,36,38–40]. In the present paper, we consider d-term superpositions ($d \geq 1$) in one dov billiards. One derives a d-dimensional Galërkin projection of the Schrödinger equation to obtain d coupled ordinary differential equations of motion for the complex amplitudes in the normal mode expansion of the wavefunction. One then uses a "generalized Bloch transformation" (GBT) to obtain equations of motion in the position, momentum, and $(d^2 - 1)$ "generalized Bloch variables" (GBVs). Using the radially vibrating spherical billiard with null angular-momentum eigenstates [39] for numerical simulations, we review the $d = 2$ case and also analyze the $d = 3$ case explicitly. We discuss the geometric aspects of this problem and briefly mention how one can generalize the present study to quantum billiards with more than one dov.

Quantum billiards describe the motion of a point particle of mass m_0 undergoing perfectly elastic collisions in a domain in a potential V with a boundary of mass $M \gg m_0$. With this condition on the mass ratio, we assume that the boundary does not recoil from collisions with the confined particle. Point particles in quantum billiards possess wavefunctions that satisfy the Schrödinger equation, whose time-independent part is the Helmholtz equation. One uses homogeneous Dirichlet boundary conditions, as the wavefunctions are constrained to vanish on the boundary [27]. It is known that globally separable quantum billiards with "stationary" (i.e., zero dov) boundaries are not chaotic but that quantum billiards with at least one dov may behave chaotically under certain conditions [40]. (A quantum billiard is *globally separable* when the geometry of the billiard is one for which the Helmholtz equation is globally

separable.) In the case of the radially vibrating spherical billiard, at least one pair of a finite-term superposition must have equal orbital (l) and azimuthal (m) quantum numbers for the system to exhibit chaotic behavior [28]. This condition is satisfied automatically if one considers only null angular-momentum eigenstates [39].

2. Galërkin expansions

Galërkin expansions are used to study semilinear partial differential equations such as reaction–diffusion equations. They can also be used, for example, to study nonlinear Schrödinger (NLS) equations. The present treatment of the linear Schrödinger equation with nonlinear boundary conditions parallels established methods for nonlinear partial differential equations, because these analyses both rely on Galërkin methods. Additionally, many finite element schemes are based on Galërkin approximations [26].

Consider a (possibly nonlinear) partial differential equation $\mathrm{O}\psi = 0$. The operator O takes the form

$$\mathrm{O} \equiv \mathrm{L} + \mathrm{N}, \tag{1}$$

where L is a linear differential operator and N a nonlinear one. (A good example to keep in mind is the NLS, as L is the Schrödinger operator in that case.) One expresses ψ as an expansion using some orthonormal set of eigenfunctions $\psi_i(x)$ of L, $i \in I$:

$$\psi(x) = \sum_I c_i(\bar{x})\psi_i(x), \quad x \in X, \tag{2}$$

where I is an indexing set and the coefficients $c_i(\bar{x})$ are unknown functions of some subset of variables $\bar{x}$ of the original vector of variables x. It is important to realize that the coefficients c_i depend only on some of the independent variables and not the entire vector x of variables. In the present paper, for example, we consider coefficients that depend only on time.

The eigenfunctions ψ_i are associated with the linear differential equation $\mathrm{L}\psi = 0$ along with a set of (linear and time-independent) boundary conditions. This yields a countably infinite coupled system of nonlinear ordinary differential equations for $c_i(\bar{x}), i \in I$ [45]. (If the partial differential equation is linear with linear boundary conditions so that $\mathrm{N} \equiv 0$, then taking an eigenfunction expansion yields constant coefficients $c_i(\bar{x}) \equiv c_i$. Otherwise, one obtains a system of nonlinear ordinary differential equations.) One then projects the expansion (2) onto a finite-dimensional subspace (by assuming that only a certain finite subset of the $c_i(\bar{x})$ are nonzero) to obtain a finite system of coupled nonlinear ordinary differential equations. (The differential equations so obtained are often called *amplitude equations* [5,25].) Thus, for example, a two-term superposition state corresponds to a two-mode Galërkin projection. If all the dynamical behavior of a system lies on such a finite-dimensional projection, then one has found an *inertial manifold* (global center manifold) that necessarily contains any global attractor that the system might have [45]. Perhaps the most famous example of a Galërkin approximation is the Lorenz model, which is a three-mode truncation of the Boussinesq equations for fluid convection in a two-dimensional layer heated from below [47].

When applying Galërkin expansions to nonlinear partial differential equations $\mathrm{O}\psi = 0$, one decomposes the operator O into (nontrivial) linear and nonlinear parts

$$\mathrm{O} \equiv \mathrm{L} + \mathrm{N} \tag{3}$$

and expands according to the eigenfunctions of the linear operator L and the relevant boundary conditions. Such methods are thus applicable to nonlinear operators that are nontrivially decomposable into linear and nonlinear parts. The term “semilinear” is often applied to operators that can be decomposed in this manner. For the NLS and

complex Ginzburg–Landau (CGL) equations, L corresponds to the linear Schrödinger operator. In this context, the study of vibrating quantum billiards is related to the study of NLS and CGL equations.

2.1. Physical interpretation of d-term Galërkin expansions

We discussed earlier that a d-term Galërkin projection corresponds to a d-term superposition state. We now consider the issue of when such a state occurs in physical systems relevant to vibrating quantum billiards. The condition under which such an approximation is valid corresponds to the case in which the other states of the system have negligible contribution to the dynamics. Because the present system cannot admit an exact inertial manifold, we justify ignoring the other modes of the system on physical grounds. The primary examples to keep in mind are polyatomic molecules with d-fold degeneracies or near-degeneracies in their electronic energy levels [46].

Molecular systems exhibit both electronic (fast) and nuclear (slow) dof. In the Born–Oppenheimer approximation [4,6,7,35], one quantizes the electronic dof and treats the (much slower) motion of the nucleus as a perturbation of electronic motion in a nucleus of constant size. One may consider molecular systems in which only d of the states give an important contribution to the dynamics of the system—that is, the system is aptly described by $(d-1)$ quantum-mechanical dof. One may do this if the d states in question have energies that are the same or are at least sufficiently close to each other so that when one considers the coupling of electronic and nuclear motion, the system may be treated semiquantally [32]. As one increases the mass of the nucleus relative to that of the electron, the electronic energy levels need not be as close together for a semiquantum description to be valid. The increased nuclear mass causes the nuclear eigenenergies to lie closer together and be more accurately approximated as a continuum for a given electronic spectrum. This continuum approximation corresponds to treating the nuclear dof classically.

The semiquantum regime aptly describes the dynamics of molecules when they undergo nonadiabatic transitions [35,46,50]. In this regime, the nuclear dof (in other words, the dov) are treated classically, whereas the electronic dof are treated quantum-mechanically [14,46]. One uses a d-term Galërkin projection when the $(d+1)$th term is far enough away that it may be ignored. As the first d electronic energy levels are either degenerate or nearly so, the use of d-mode Galërkin expansions allows one to explore the nonadiabatic transitions involving their associated eigenstates [7,35]. Ordinarily, one encounters near-degeneracies involving very few eigenstates. This, then, provides a rationale for the analysis of few-mode Galërkin expansions and the resulting low-dimensional systems of ordinary differential equations. Additionally, this provides a physical meaning to vibrating quantum billiards: a d-mode superposition state of an s dov quantum billiard describes nonadiabatic transitions in a polyatomic molecule with s excited nuclear modes and a d-fold electronic near-degeneracy. These transitions resemble the Jahn–Teller effect [7,35,46,50]. A common reason for degeneracy and near-degeneracy of electronic energy levels is molecular symmetry. Indeed, we found in a previous study that vibrating quantum billiards require certain symmetries for different eigenstates to couple with each other [40].

As the semiquantum treatment of vibrating quantum billiards yields a conservative Hamiltonian system (as we discuss in detail later), d-mode Galërkin expansions cannot capture their exact mathematical behavior. As just discussed, however, taking few-mode Galërkin expansions is justified on physical grounds. Additionally, the fact that some dynamical behavior is ignored with this process also has a physical interpretation: the complexity of nonadiabatic transitions increases markedly as the number of degenerate or nearly degenerate eigenstates increases. As we shall see, applying Galërkin projections to vibrating quantum billiards is an insightful and convenient mathematical formalism for the study of nonadiabatic dynamics in semiquantum systems. Finally, note that Galërkin expansions correspond to what researchers in quantum mechanics have done for years when they restrict themselves to d electronic energy levels.

3. One-term expansions

Consider a one dov quantum billiard on a Riemannian manifold (X, g). Suppose we have isolated the nth normal mode of the present system. Insert the wavefunction

$$\psi(x,t) = \psi_n(x,t;a(t)) \tag{4}$$

into the time-dependent Schrödinger equation

$$\mathrm{i}\hbar\frac{\partial\psi(x,t)}{\partial t} = K\psi(x,t) = -\frac{\hbar^2}{2m}\nabla^2\psi(x,t), \quad x \in X, \tag{5}$$

where the electronic kinetic energy is given by

$$K = -\frac{\hbar^2}{2m}\nabla^2, \tag{6}$$

where $a \equiv a(t)$ represents the time-varying boundary component (e.g., the radius in the radially vibrating spherical billiard). The total molecular Hamiltonian of the system is given by

$$H(a,P) = K + \frac{P^2}{2M} + V, \tag{7}$$

where the walls of the quantum billiard are in a potential V and have momentum P with corresponding mass M. For the present configuration, we assume that V does not depend explicitly on time. That is,

$$V = V(a) \tag{8}$$

depends only on the nuclear coordinate a.

Vibrating quantum billiards have time-dependent (nonlinear) boundary conditions:

$$\psi(a(t)) = 0, \quad t \in \mathbb{R}, \tag{9}$$

which is why one may use Galërkin projections to study them. As discussed earlier, this corresponds to a procedure that may be used to study nonlinear partial differential equations such as reaction–diffusion equations and NLS equations [45]. As the time-dependence of $a(t)$ in Eq. (9) is unknown, the problem of interest is said to have a free boundary [18]. To solve the Schrödinger equation with Dirichlet boundary conditions in this situation, one must determine the form of $a(t)$, which plays the role of a lengthscale in the vibrating quantum billiard's eigenfunctions (see Appendix A). Applying a Galërkin method to this problem yields a set of ordinary differential equations that determine the time-dependence of $a(t)$, its conjugate momentum $P(t)$, and the quantum-mechanical variables [40]. Perhaps the simplest example to visualize is the radially vibrating spherical quantum billiard, in which the domain X of the Schrödinger equation is

$$X = \{r \in \mathbb{R}^3 | r \leq a(t)\}. \tag{10}$$

The time-dependence in the definition of the domain of interest (10) leads to the use of Galërkin projections in the study of vibrating quantum billiards. The fact that the potential V (8) does not depend explicitly on time, as it does in the work of other researchers who study similar problems [3,10,12,33,42], is also important for the application of a Galërkin approach. As V depends only on a, it may be treated as a constant when using a Galërkin expansion to derive amplitude equations from Schrödinger's equation (5).

When considering a single eigenstate, there is only one probability, $|A_n|^2 \equiv 1$, as we are projecting the system onto a one-dimensional subspace. Physically, this corresponds to a situation in which electronic energies are far

enough away from each other so that different eigenstates do not mix (couple) with each other. In terms of billiards, this corresponds to a situation in which the boundary is uncoupled from the enclosed particle, so one obtains a system whose dynamics correspond to the classical ("Ehrenfest") motion of the wall [35,46]. The quantum-mechanical wavefunction ψ nevertheless depends on these classical dynamics, as the wave changes nontrivially with the nuclear coordinate a. For example, the energy associated with the wave fluctuates with the displacement a. (The kinetic energy of the particle becomes smaller when a increases and vice versa.) Put simply, even without mutual coupling between quantum and classical components, the quantum dynamics depend nontrivially on the classical motion of the boundary. There is thus a sort of "enslavement" of the quantum subsystem by the classical subsystem, as the classical motion is unaffected by the dynamics of the confined particle.

The present system, in other words, is a Hamiltonian system whose equations of motion are given by

$$\dot{a} = \frac{P}{M} \equiv \frac{\partial H}{\partial P}, \qquad \dot{P} = -\frac{\partial V}{\partial a} + \frac{2\epsilon_n}{a^3} \equiv -\frac{\partial H}{\partial a}, \tag{11}$$

where ϵ_n is the energy parameter corresponding to the nth eigenstate [40]. (The influence of the quantum subsystem on the classical one is encompassed entirely by the size of the parameter ϵ_n. There is no feedback.) Equilibria of this system satisfy $P = 0$ and

$$\frac{\partial V}{\partial a}(a_*) = \frac{2\epsilon_n}{a_*^3}, \tag{12}$$

where a_* is an equilibrium displacement. In a previous study [36], we analyzed the bifurcation structure of (11). One inserts the dynamics of $a(t)$ into the wave $\psi(x, t; a(t))$, which may be termed a *nonlinear normal mode* because of its dependence on a. As the Hamiltonian system (11) has one dof, it is necessarily integrable. Thus, the normal mode we obtained is not chaotic. Nevertheless, even in this degenerate case, the quantum dynamics depend on the classical dynamics.

4. Two-term expansions

We now review previous analysis of two-term superposition states [28,39,40]. The superposition of the nth and qth states is given by

$$\psi_{nq}(x, t) \equiv A_n(t)\psi_n(x, t) + A_q(t)\psi_q(x, t), \tag{13}$$

which we substitute into the time-dependent Schrödinger equation (5). Taking the expectation of both sides of (5) for the state (13) yields the following relations:

$$\begin{aligned} &\left\langle \psi_{nq} \left| -\frac{\hbar^2}{2m}\nabla^2\psi_{nq} \right\rangle = K(|A_n|^2, |A_q|^2, a_1, \ldots, a_s), \right. \\ &\mathrm{i}\hbar \left\langle \psi_{nq} \left| \frac{\partial \psi_{nq}}{\partial t} \right\rangle = \mathrm{i}\hbar[\dot{A}_n A_q^* + \dot{A}_q A_n^* + \nu_{nn}|A_n|^2 + \nu_{qq}|A_q|^2 + \nu_{nq}A_n A_q^* + \nu_{qn}A_q A_n^*]. \right. \end{aligned} \tag{14}$$

If the billiard has one dov, then the electronic kinetic energy is given by

$$K = K(|A_n|^2, |A_q|^2, a). \tag{15}$$

Defining $A_1 \equiv A_n$ and $A_2 \equiv A_q$, the quadratic form (14) yields the amplitude equations

$$\mathrm{i}\dot{A}_k = \sum_{j=1}^{2} D_{kj}A_j, \tag{16}$$

where

$$D \equiv D_{kj} = \begin{pmatrix} \dfrac{\epsilon_n}{\hbar a^2} & -\mathrm{i}\mu_{nq}\dfrac{\dot{a}}{a} \\ \mathrm{i}\mu_{nq}\dfrac{\dot{a}}{a} & \dfrac{\epsilon_q}{\hbar a^2} \end{pmatrix}, \tag{17}$$

and $\mu_{nq} = -\mu_{qn} \not\equiv 0$ is a coupling coefficient for the cross term $A_n A_q^*$. The coefficient μ_{nq} is defined by the relation

$$\nu_{nq} \equiv \frac{\dot{a}}{a}\mu_{nq}, \tag{18}$$

and for the special case of null angular-momentum eigenstates of the radially vibrating spherical, is given by the expression

$$\mu_{nq} = 2\frac{qn}{(n+q)(q-n)}, \quad n < q. \tag{19}$$

We remark that in this case, $\mu_{nq} > 0$ provided that $n < q$.

If the coupling coefficient μ_{nq}, which describes the strength of the interaction between the nth and qth eigenstates, vanishes in a one dov quantum billiard, then the two eigenstates under consideration do not couple with each other. We showed in a previous study that whether or not two states in vibrating quantum billiards couple with each other depends only on their relative quantum numbers [40]. If they are not coupled, the situation corresponds mathematically to that obtained with one-term superposition states. That is, the classical equations of motion for the billiard boundary take the same form, except that the electronic kinetic energy is different. The quantum dynamics of the particle enclosed by the boundary is enslaved to the classical motion of the walls but does not itself affect that motion (aside from determining the values of the energy parameters ϵ_j). We hence assume the interaction strength is nonzero so that we have a new dynamical situation to discuss.

Transforming the amplitude equations (16) using Bloch variables (see Eq. (B.6)) yields the following equations of motion:

$$\begin{aligned} &\dot{x} = -\frac{\omega_0 y}{a^2} - \frac{2\mu_{nq}Pz}{Ma}, \qquad \dot{y} = \frac{\omega_0 x}{a^2}, \qquad \dot{z} = \frac{2\mu_{nq}Px}{Ma}, \\ &\dot{a} = \frac{P}{M}, \qquad \dot{P} = -\frac{\partial V}{\partial a} + \frac{2[\epsilon_+ + \epsilon_-(z - \mu_{nq}x)]}{a^3}. \end{aligned} \tag{20}$$

In (20),

$$\omega_0 \equiv \frac{\epsilon_q - \epsilon_n}{\hbar}, \tag{21}$$

and

$$\epsilon_\pm \equiv \tfrac{1}{2}(\epsilon_n \pm \epsilon_q), \tag{22}$$

where ϵ_n and ϵ_q $(n < q)$ are the coefficients in the kinetic energy.

The equilibria for the dynamical system (20) satisfy $x = y = 0$, $z = \pm 1$, $a = a_*$, and $P = 0$, where the equilibrium radii $\{a_*\}$ are solutions of the equation

$$\frac{\partial V}{\partial a}(a_*) = \frac{2}{a_*^3}(\epsilon_+ \pm \epsilon_-), \tag{23}$$

so that

$$\frac{\partial V}{\partial a}(a_*) = \frac{2\epsilon_j}{a_*^3}, \quad j \in \{1, 2\}. \tag{24}$$

For the harmonic potential

$$V(a) = \frac{V_0}{a_0^2}(a - a_0)^2, \tag{25}$$

one obtains equilibrium radii $a_\pm$ that satisfy

$$a - a_0 = \frac{\epsilon_k a_0^2}{V_0 a^3}, \quad k \in \{n, q\}, \tag{26}$$

where the subscript $\pm$ corresponds to $z = \pm 1$. When $z = +1$, the system is entirely in the qth state, whereas when $z = -1$, the system is entirely in the nth state. One may show that each of the present system's equilibria are elliptic as long as $V(a)+K(a)$ has a single minimum with respect to a. That is, every eigenvalue of the Jacobian of the linearized system is purely imaginary. For the system at hand, one eigenvalue is identically zero—corresponding to the row in the Jacobian matrix arising from the derivatives of $\dot{z}(a, P, x, y, z) \equiv f_3(a, P, x, y, z)$—and the other four constitute two pure imaginary complex conjugate pairs when this ellipticity condition is satisfied. When this condition is not satisfied (such as with a double-well potential V with a suitably large central mound), one observes generalizations of saddle-center bifurcations [36]. Moreover, different potentials $V(a)$ may exhibit additional equilibria, although each of them corresponds to the manifestation of a single normal mode. However, as the energy of the normal mode varies with the displacement a, we may obtain several different pure state equilibria corresponding to the same state (such as the ground state), but with a different frequency and energy because it is associated with a different equilibrium value of the nuclear displacement a. This occurs only when at least one of the equilibria violates the ellipticity condition, so one cannot guarantee the stability of these new equilibria a priori.

The five-dimensional dynamical equations (20) exhibit quantum chaos for some initial conditions, as can be seen in Poincaré sections in the (a, P)-plane (Fig. 1) and the (x, y)-plane (Fig. 2) as long as the fixed-boundary (fb) quantum numbers of the two superposition states are the same [40]. (This occurs exactly when μ_{nq} is nonzero.) We used the harmonic potential for both plots. As discussed in prior works [28,40], one has a classically chaotic subsystem (described by the Hamiltonian variables a and P) coupled to a quantum chaotic subsystem (described by the Bloch variables x, y, and z). The present system is thus semiquantum chaotic [9]. We note that unlike with one-term Galërkin projections, the normal modes ψ_n and ψ_q are not only nonlinear but also chaotic (because the radius $a(t)$ behaves chaotically). Such wave chaos in a quantum system is a signature of semiquantum chaos.

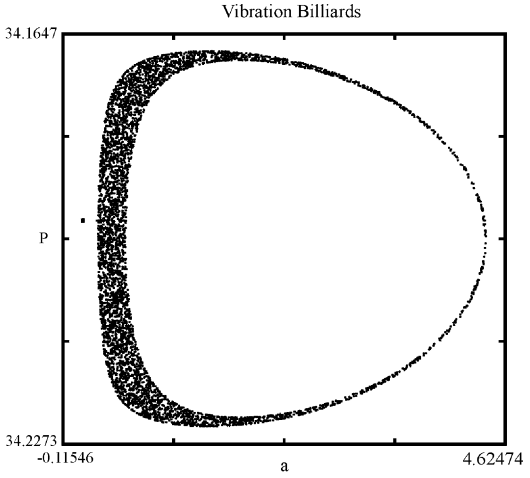

Fig. 1. Poincaré section for the cut $x = 0$ in the (a, P)-plane.

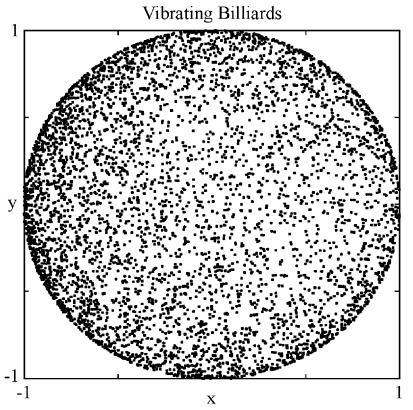

Fig. 2. Poincaré section for the cut $P = 0$ projected into the (x, y)-components of the Bloch sphere.

5. Three-term expansions

Let us now extend our analysis to three-term superposition states. Insert the wave

$$\psi_{(3)}(x,t) \equiv A_{n_1}(t)\psi_{n_1}(x,t) + A_{n_2}(t)\psi_{n_2}(x,t) + A_{n_3}(t)\psi_{n_3}(x,t), \tag{27}$$

which is a superposition of n_1, n_2, and n_3 eigenstates, into the Schrödinger equation (5). Taking the expectation of both sides of (5) for the state (27) of a one dov quantum billiard yields

$$\begin{aligned}
\left\langle \psi_{(3)} \left| -\frac{\hbar^2}{2m}\nabla^2\psi_{(3)} \right\rangle \right. &= K(|A_{n_1}|^2, |A_{n_2}|^2, |A_{n_3}|^2, a),\\
\mathrm{i}\hbar\left\langle \psi_{(3)} \left| \frac{\partial\psi_{(3)}}{\partial t} \right\rangle \right. &= \mathrm{i}\hbar[\dot{A}_{n_1}A^*_{n_2} + \dot{A}_{n_1}A^*_{n_3} + \dot{A}_{n_2}A^*_{n_1}\dot{A}_{n_2}A^*_{n_3} + \dot{A}_{n_3}A^*_{n_1} + \dot{A}_{n_3}A^*_{n_2} + \nu_{n_1n_1}|A_{n_1}|^2\\
&\quad + \nu_{n_2n_2}|A_{n_2}|^2 + \nu_{n_3n_3}|A_{n_3}|^2 + \nu_{n_1n_2}A_{n_1}A^*_{n_2} + \nu_{n_1n_3}A_{n_1}A^*_{n_3} + \nu_{n_2n_1}A_{n_2}A^*_{n_1}\\
&\quad + \nu_{n_2n_3}A_{n_2}A^*_{n_3} + \nu_{n_3n_1}A_{n_3}A^*_{n_1} + \nu_{n_3n_2}A_{n_3}A^*_{n_2}]\\
&= \mathrm{i}\hbar\left[\sum_{i,j=1,i\neq j}^{3}\dot{A}_{n_i}A^*_{n_j} + \sum_{i=1}^{3}\nu_{n_in_i}|A_{n_i}|^2 + \sum_{i,j=1,i\neq j}^{3}\nu_{n_in_j}A_{n_i}A^*_{n_j}\right].
\end{aligned} \tag{28}$$

Denoting A_{n_j} as A_j, the quadratic form (28) gives

$$\mathrm{i}\dot{A}_k = \sum_{j=1}^{3} D_{kj}A_j, \tag{29}$$

where

$$D = D_{kj} = \begin{pmatrix} \dfrac{\epsilon_1}{\hbar a^2} & -\mathrm{i}\mu_{12}\dfrac{\dot{a}}{a} & -\mathrm{i}\mu_{13}\dfrac{\dot{a}}{a}\\ \mathrm{i}\mu_{12}\dfrac{\dot{a}}{a} & \dfrac{\epsilon_2}{\hbar a^2} & -\mathrm{i}\mu_{23}\dfrac{\dot{a}}{a}\\ \mathrm{i}\mu_{13}\dfrac{\dot{a}}{a} & \mathrm{i}\mu_{23}\dfrac{\dot{a}}{a} & \dfrac{\epsilon_3}{\hbar a^2} \end{pmatrix}, \tag{30}$$

the parameter $\epsilon_j \equiv \epsilon_{n_j}$ is the jth energy coefficient, and $\mu_{ij} \equiv \mu_{n_i n_j} = -\mu_{n_j n_i} \not\equiv 0$ is a coupling coefficient for the cross term $A_{n_i} A^*_{n_j}$ (which is defined as before). The interaction strength μ_{ij} is nonzero when the fb quantum numbers of the n_ith and n_jth states are the same. When coupling coefficients vanish, the situation reduces to ones examined previously. If they all vanish, the present system is integrable. If two sets of them vanish (because one of the eigenstates has a different set of fb quantum numbers than the other two), then the dynamics of the present system corresponds to that for two-term superposition states. We thus assume without loss of generality that none of the coupling coefficients vanish, so that we are considering a new physical situation.

We transform the amplitudes $|A_1|^2$, $|A_2|^2$, and $|A_3|^2$ using a GBT (see Appendix B). This yields nine variables and five constraints, which implies that the system has two independent quantum-mechanical dof. One can also count these dof in a different manner. The present situation involves three complex amplitudes A_i, corresponding to six real variables. The sum of their squares is unity (by conservation of probability) and the dynamics of the present system are invariant under global phase shifts. Consequently, there are four independent real variables and hence two dof.

Using GBVs, the kinetic energy may be expressed as

$$K = \frac{2}{3a^2}([z_{12}\epsilon^-_{12} + z_{13}\epsilon^-_{13} + z_{23}\epsilon^-_{23}] + \epsilon_+) = \frac{2}{3a^2}([z_{12}\epsilon^-_{12} + (z_{12}+z_{23})\epsilon^-_{13} + z_{23}\epsilon^-_{23}] + \epsilon_+), \tag{31}$$

where

$$\epsilon^-_{kl} \equiv \tfrac{1}{2}(\epsilon_l - \epsilon_k) \tag{32}$$

as before and

$$\epsilon^+ \equiv \tfrac{1}{2}(\epsilon_k + \epsilon_l + \epsilon_m). \tag{33}$$

The equations of motion describing this three-term superposition states are thus

$$\begin{aligned}
\dot{x}_{12} &= -\frac{\omega_{12}}{a^2} y_{12} - \frac{2\mu_{12} P z_{12}}{Ma} - \frac{P}{Ma}[\mu_{23}x_{13} + \mu_{13}x_{23}],\\
\dot{x}_{13} &= -\frac{\omega_{13}}{a^2} y_{13} - \frac{2\mu_{13} P (z_{12}+z_{23})}{Ma} + \frac{P}{Ma}[\mu_{23}x_{12} - \mu_{12}x_{23}],\\
\dot{x}_{23} &= -\frac{\omega_{23}}{a^2} y_{23} - \frac{2\mu_{23} P z_{23}}{Ma} + \frac{P}{Ma}[\mu_{13}x_{12} + \mu_{12}x_{13}],
\end{aligned} \tag{34}$$

$$\begin{aligned}
\dot{y}_{12} &= \frac{\omega_{12}x_{12}}{a^2} + \frac{P}{Ma}[\mu_{13}y_{23} - \mu_{23}y_{13}], \qquad \dot{y}_{13} = \frac{\omega_{13}x_{13}}{a^2} + \frac{P}{Ma}[\mu_{23}y_{12} - \mu_{12}y_{23}],\\
\dot{y}_{23} &= \frac{\omega_{23}x_{23}}{a^2} + \frac{P}{Ma}[\mu_{12}y_{13} - \mu_{13}y_{12}],
\end{aligned} \tag{35}$$

$$\dot{z}_{12} = \frac{2\mu_{12}Px_{12}}{Ma} + \frac{P}{Ma}[\mu_{13}x_{13} - \mu_{23}x_{23}], \qquad \dot{z}_{23} = \frac{2\mu_{23}Px_{23}}{Ma} + \frac{P}{Ma}[\mu_{13}x_{13} - \mu_{12}x_{12}], \tag{36}$$

$$\dot{a} = \frac{P}{M} \equiv \frac{\partial H}{\partial P}, \qquad \dot{P} = -\frac{\partial V}{\partial a} - \frac{\partial K}{\partial a} \equiv -\frac{\partial H}{\partial a}, \tag{37}$$

where

$$\begin{aligned}
\frac{\partial K}{\partial a} = &-\frac{4\epsilon^+}{3a^3} - \frac{4}{3a^3}[z_{12}\epsilon^-_{12} + (z_{12}+z_{23})\epsilon^-_{13} + z_{23}\epsilon^-_{23}] + \frac{2}{3a^3}\epsilon^-_{12}(2\mu_{12}x_{12} + \mu_{13}x_{13} - \mu_{23}x_{23})\\
&+\frac{2}{3a^3}\epsilon^-_{13}(\mu_{12}x_{12} + 2\mu_{13}x_{13} + \mu_{23}x_{23}) + \frac{2}{3a^3}\epsilon^-_{23}(-\mu_{12}x_{12} + \mu_{13}x_{13} + 2\mu_{23}x_{23})
\end{aligned} \tag{38}$$

since

$$\frac{\partial z_{12}}{\partial a} = \frac{\partial z_{12}}{\partial t}\frac{\partial t}{\partial a} \equiv \frac{\dot{z}_{12}}{\dot{a}} = \frac{2\mu_{12}x_{12}}{a} + \frac{1}{a}[\mu_{13}x_{13} - \mu_{23}x_{23}],$$
$$\frac{\partial z_{23}}{\partial a} = \frac{\partial z_{23}}{\partial t}\frac{\partial t}{\partial a} \equiv \frac{\dot{z}_{23}}{\dot{a}} = \frac{2\mu_{23}x_{23}}{a} + \frac{1}{a}[\mu_{13}x_{13} - \mu_{12}x_{12}]. \tag{39}$$

Additionally, recall that

$$\omega_{kl} \equiv \frac{\epsilon_l - \epsilon_k}{\hbar}. \tag{40}$$

The equilibria of the present 10-dimensional dynamical system (37) satisfy $P = 0$, $x_{ij} = y_{ij} = 0$, $z_{12}^2 + z_{12}z_{23} + z_{23}^2 = 1$, and

$$\frac{\partial V}{\partial a} = \frac{4}{3a^3}[\epsilon^+ + z_{12}\epsilon_{12}^- + (z_{12} + z_{23})\epsilon_{13}^- + z_{23}\epsilon_{23}^-]. \tag{41}$$

Applying the constraints (B.11) with $x_{ij} = y_{ij} = 0$ shows that there are three possible sets of values for the z-Bloch variables:

$$(z_{12}, z_{13} \equiv z_{12} + z_{23}, z_{23}) = (0, 1, 1), (1, 0, -1), (-1, -1, 0). \tag{42}$$

Each of these equilibria corresponds to one type of pure state, as expected from our physical intuition. Let us consider each of these in turn. If $z_{12} = 0$, then $|A_1|^2 = |A_2|^2 = 0$ and $|A_3|^2 = 1$, so the only state present is the third one. If $z_{13} = 0$, then only the state with complex amplitude A_2 gives a nonvanishing contribution. Finally, for $z_{23} = 0$, only the first pure state is present. When only the jth state is present at equilibrium, it has kinetic energy

$$E_j = \frac{\epsilon_j}{a_*^2}, \tag{43}$$

where a_* is the equilibrium radius. This, therefore, corresponds to the expected generalization from two-state systems to three-state systems. The relation (41) becomes

$$\frac{\partial V}{\partial a}(a_*) = \frac{2\epsilon_j}{a^3}, \quad j \in \{1, 2, 3\}, \tag{44}$$

which is the exact equilibrium relation we derived for one-term and two-term superposition states. The total number of equilibria depends on the form of the external potential $V(a)$ just as for two-term Galërkin projections. That is, $V(a)$ determines the number of equilibrium radii for each pure state equilibrium. Mixed-state equilibria cannot occur.

When calculating the eigenvalues of the present system's equilibria, the degree-10 characteristic polynomial always has two zero roots that factor out. This follows from the equations of motion for the z-Bloch variables. One then factors the remaining degree-8 polynomial to determine the nontrivial eigenvalues. The present system is Hamiltonian, so the remaining polynomial is a degree-4 polynomial in λ^2. Moreover, as this system has three dof, its equilibria have only three eigenvalues that give independent information. An equilibrium is elliptic whenever each of its associated square eigenvalues λ^2 is negative. We may conclude by physical considerations (although we will not prove this rigorously) that—just as for two-term superposition states—all the equilibria are elliptic provided the quantity

$$E \equiv V(a) + K(z_{ij}, a) \tag{45}$$

has a single minimum with respect to the displacement a. When this happens, the time-derivative of the momentum P vanishes exactly once if one varies a quasistatically by holding the z-Bloch variables (and hence the probability amplitudes A_j) constant. In this event, there is exactly one configuration of the boundary corresponding to each pure state

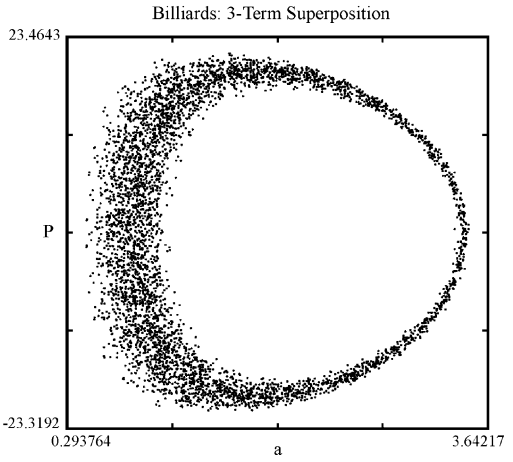

Fig. 3. Poincaré section for the cut $x_{12} = 0$ in the (a, P)-plane for a three-term superposition state. This plot shows fully chaotic regions similar to those often observed in two-term superpositions.

equilibrium. If there were some sort of saddle structure (equivalently, if one or more of the equilibria were not elliptic), then $\dot{P}$ would necessarily vanish at multiple displacements a_* for each of the normal modes in question. The transitions in question are generalizations of saddle-center bifurcations, as shown explicitly for two-term superposition states in a previous work [36]. (For one-term superposition states, one obtains canonical saddle-center bifurcations.)

We investigate the dynamics of Eq. (37) numerically when the billiard resides in the harmonic potential

$$V(a) = \frac{V_0}{a_0^2}(a - a_0)^2, \tag{46}$$

for which all equilibria are elliptic since the electronic kinetic energy K is positive definite. As expected, the behavior of the present system is more intricate than that observed in two-term superposition states. For some choices of parameters and initial conditions, however, one obtains plots whose dynamics are very similar to those for two-term superpositions. Figs. 3–15 display plots exemplifying the dynamics of a three-term superposition consisting of the ground state and the first two null angular-momentum $(l = 0, m = 0)$ excited states of the radially vibrating

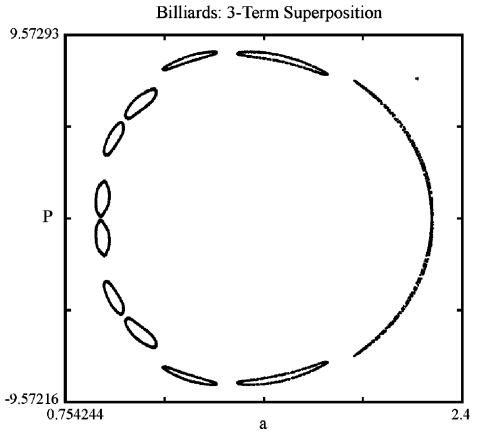

Fig. 4. Poincaré section for the cut $x_{12} = 0$ in the (a, P)-plane for a three-term superposition state.

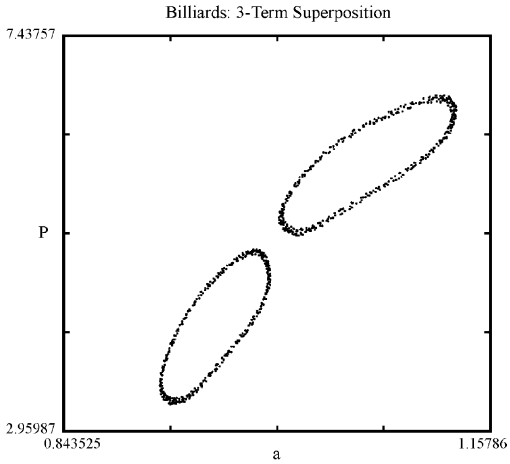

Fig. 5. A closer look at part of the Poincaré section for the cut $x_{12} = 0$ in the (a, P)-plane for a three-term superposition state.

spherical quantum billiard. We used the parameter values $\hbar = 1$, $M = 10$, $m = 1$, $\epsilon_1 = \pi^2/2m \approx 4.9348022$, $\epsilon_2 = 4\pi^2/2m \approx 19.7392088$, $\epsilon_3 = 9\pi^2/2m \approx 44.4132198$, $V_0/a_0^2 = 5$, and $a_0 = 1.25$. The resultant coupling coefficients are $\mu_{12} = 4/3$, $\mu_{13} = 3/4$, and $\mu_{23} = 12/5$. Fig. 3 shows a Poincaré map (of the cut $x_{12} = 0$) projected into the (a, P)-plane. The initial conditions for this plot are $x_{12}(0) = \sin(0.95\pi) \approx 0.156434$, $x_{13}(0) = x_{23}(0) = 0$, $y_{12}(0) = y_{13}(0) = y_{23}(0) = 0$, $z_{12}(0) = \cos(0.95\pi) \approx -0.987688$, $z_{23}(0) = 0$, $a(0) \approx 3.3774834$, and $P(0) \approx 7.2847682$. In subsequent figures, we alter only the initial radius and conjugate momentum. The initial values of the Bloch variables correspond to those used in a previous study of two-term superposition states [28,39].

Fig. 4 shows the $x_{12} = 0$ Poincaré map projected into the (a, P)-plane. The initial radius is $a(0) \approx 2.2095438$, and the initial momentum is $P(0) \approx 3.6672913$. The dynamics in this figure are almost integrable, but a closer look reveals chaotic characteristics (see Fig. 5). There is evidence that this trajectory is near an orbit with period 6, although an additional plot reveals that another of its dof has departed quite a bit from a periodic or even

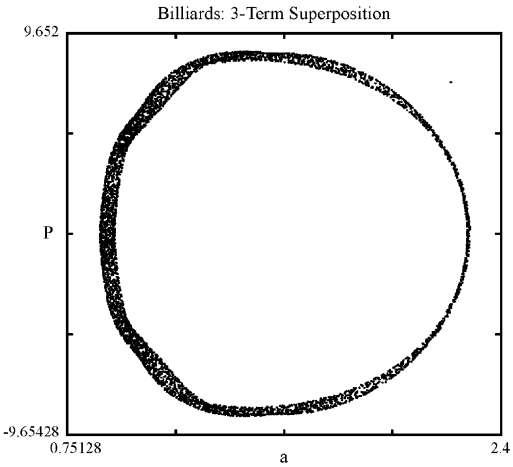

Fig. 6. Poincaré section for the cut $x_{23} = 0$ in the (a, P)-plane for a three-term superposition state. The initial conditions are the same as for Fig. 4.

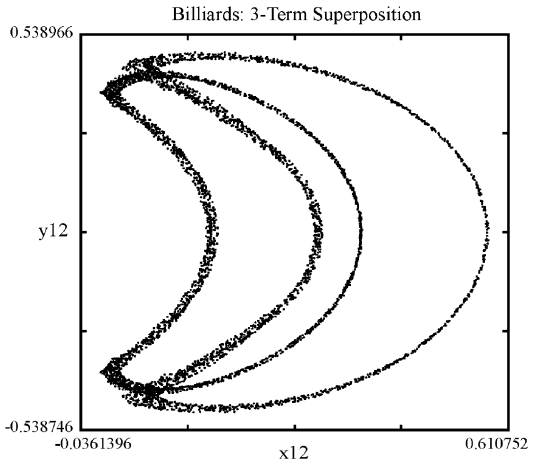

Fig. 7. Poincaré section for the cut $P = 0$ in the (x_{12}, y_{12})-plane for a three-term superposition state. The initial conditions are the same as for Fig. 4.

quasiperiodic configuration. Fig. 6 shows the $x_{23} = 0$ Poincaré cut for the same initial conditions. The chaotic behavior in this plot is less ordered, which demonstrates a different level of "excitation" corresponding to different coupling coefficients and hence to different *fundamental coupling modes* of the system. (We use the term "mode" loosely in the present context. We are not referring to the eigenmodes of the wavefunction.) The Poincaré maps for $y_{ij} = 0$ show behavior similar to that of the corresponding $x_{ij} = 0$ cut. Fig. 7 shows the $P = 0$ Poincaré map projected into the (x_{12}, y_{12})-plane of the Bloch ellipsoid. Fig. 8 is the same configuration projected into the (x_{13}, y_{13})-plane. Notice that this latter figure appears to be have departed further from an integrable configuration than the former one. Again, different coupling modes can experience different degrees of excitation or departure from integrability. That is, a d dof system may exhibit different levels of chaotic structure in its different fundamental coupling modes, each one of which represents the interaction of one pure eigenstate with another. Hence, for $d = 3$, we have three modes in this sense, corresponding to the three possible twofold interactions between the eigenstates ψ_j. It is possible that an action–angle analysis of the present system will illuminate these features.

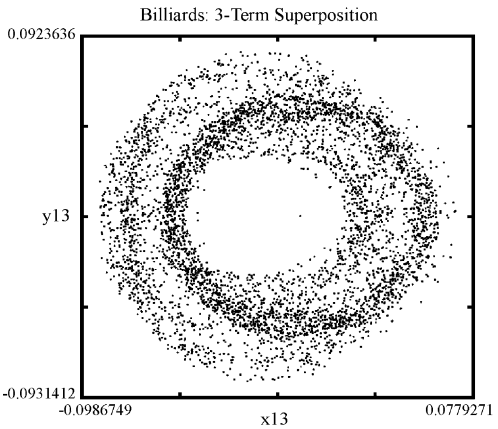

Fig. 8. Poincaré section for the cut $P = 0$ in the (x_{13}, y_{13})-plane for a three-term superposition state. The initial conditions are the same as for Fig. 4.

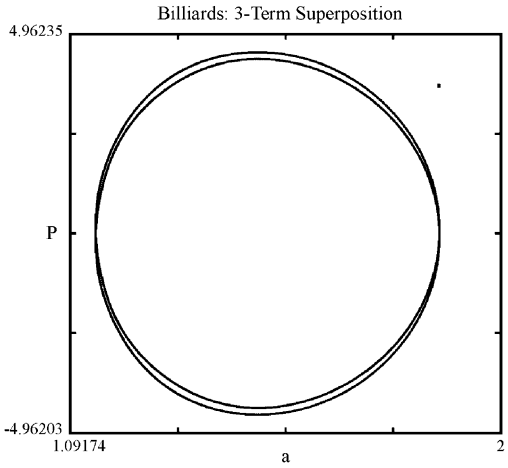

Fig. 9. Poincaré section for the cut $x_{12} = 0$ in the (a, P)-plane for a three-term superposition state. The behavior in the plot appears quasiperiodic.

Fig. 9 shows a $x_{12} = 0$ Poincaré cut in the (a, P)-plane corresponding to the initial conditions $a(0) \approx 1.8685499$ and $P(0) \approx 0.6140458$. It appears to display quasiperiodic motion, but a portion of the same plot suggests that it is not quite integrable (see Fig. 10). KAM theory also implies that this is the case, as any nonzero perturbation from an integrable configuration will cause some chaos (although it may be so small as to be impossible to resolve numerically) [19,48]. Moreover, a close-up of the same plot in the (z_{12}, z_{23})-plane (Fig. 11) reveals chaotic behavior in the Bloch variables. Unlike the classical variables, the z-Bloch variables appear to have departed quite a bit from integrability. Hence, we see that it is possible for the classical variables to behave in a nearly integrable fashion, while the quantum variables behave quite chaotically. In principle, moreover, we expect that a parameter regime can be found in which the quantum subsystem is very chaotic and the classical subsystem is almost completely integrable. (In close-ups of most regions of Fig. 9, in fact, the behavior still appears to be integrable.) In such regimes, the eigenstates (which depend on the nuclear variable a) will appear integrable in simulations of trajectories and

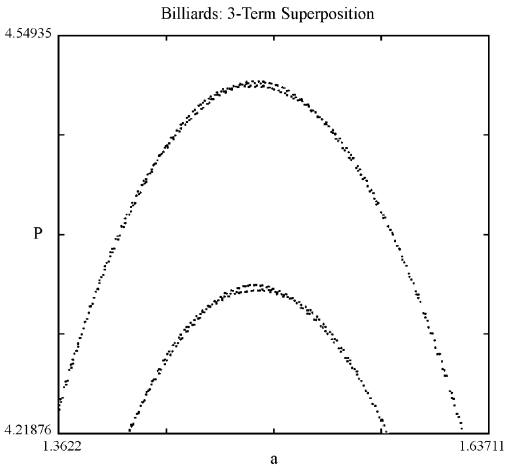

Fig. 10. A close-up of a portion of the Poincaré section for the cut $x_{12} = 0$ in the (a, P)-plane for a three-term superposition state that was shown in Fig. 9. This zoomed view reveals a small region which suggests that there may be some chaotic behavior.

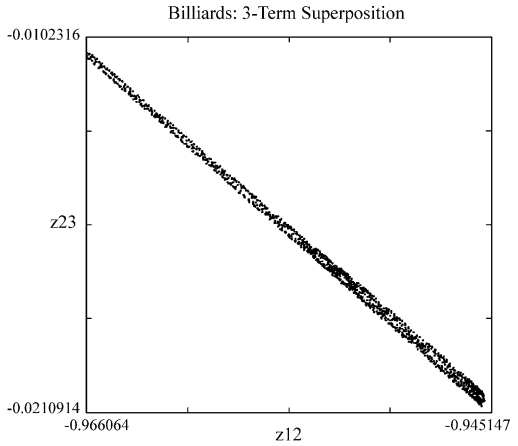

Fig. 11. Poincaré section for the cut $x_{12} = 0$ in the (z_{12}, z_{23})-plane for a three-term superposition state. The behavior in the plot displays chaos.

Poincaré sections, whereas their probabilities of expression exhibit chaotic structure. That is for d-fold electronic near-degeneracies with $d \geq 3$, one may simultaneously observe a chaotic electronic structure and a nuclear structure that cannot be distinguished in practice from being integrable. Further plots suggest that the present configuration is almost integrable with respect to the coupling between the ground state and first excited states but chaotic with respect to the other couplings. A Poincaré section in the (a, P)-plane corresponding to the cut $x_{23} = 0$ (Fig. 12) reveals chaotic characteristics, lending further credence to this possibility. Time series (Figs. 13–15) suggest the same phenomenon. Time series for the corresponding y-Bloch variables reveal similar features, whereas time series for the radius and momentum reveal motion that is almost regular. Based on the observed behavior of the classical and quantum-mechanical dof, it seems that this configuration is one for which the only irregularities of the dynamics of the radius and the momentum are ones that are extremely difficult to observe numerically. In turn, the eigenfunctions are very regular. Nevertheless, there is some chaotic structure due to the coupling between the first and second excited electronic states. The presence of a triple electronic near-degeneracy has given rise to a situation in which the ground state is almost integrable but the interaction of the two excited states is not.

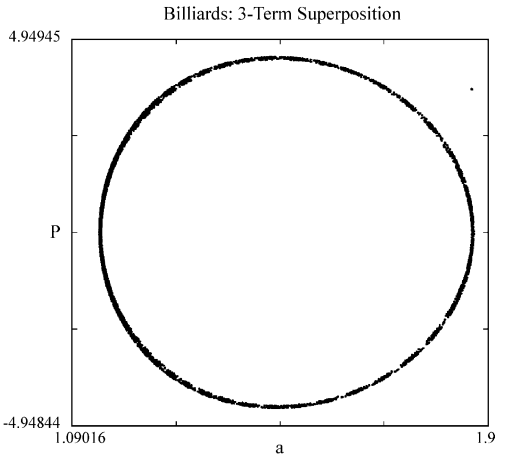

Fig. 12. Poincaré section for the cut $x_{23} = 0$ in the (a, P)-plane for a three-term superposition state. The behavior in the plot displays chaos.

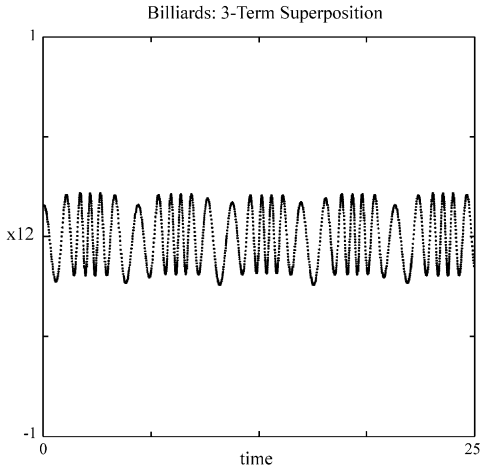

Fig. 13. Time series in $x_{12}(t)$ from $t = 0$ to 25 revealing near-integrable behavior.

Though we often observe plots that show similar features as those from two-term superposition, the dynamics of the present case are far more complicated. We have already discussed, for example, the simultaneous occurrence of regular and chaotic behavior corresponding to different fundamental interactions (coupling modes). The present system has three coupling coefficients $\{\mu_{12}, \mu_{13}, \mu_{23}\}$ rather than only one. Each of these coefficients corresponds to an interaction between two of the system's normal modes. There are parameter values and initial conditions for which some of these interactions are "excited" (chaotic) and others are not. Hence, the present system has three fundamental interactions rather than one. If one of them is "excited", one observes chaotic behavior. (Only two of these relative frequencies are independent.) This leads naturally to the notion of the *commensurability* of normal modes (eigenstates), which generalizes the use of this term in the context of oscillators. In general, two frequencies are called "commensurate" when their ratio is rational. In the canonical example of geodesic (constant velocity) motion on a torus (and hence also for constant velocity motion on a stationary rectangular billiard), the angle of the motion with respect to the base of the rectangle is determined by the relative frequency (and hence speed)

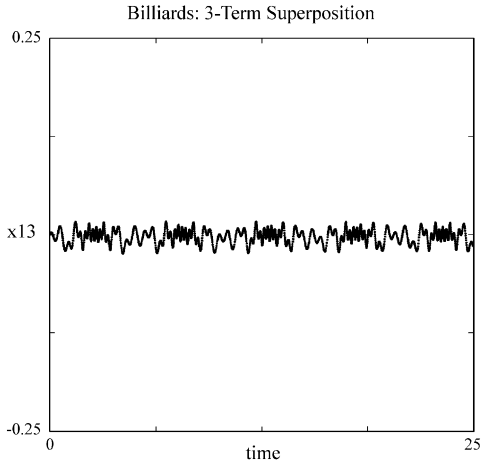

Fig. 14. Time series in $x_{13}(t)$ from $t = 0$ to 25 revealing chaotic behavior.

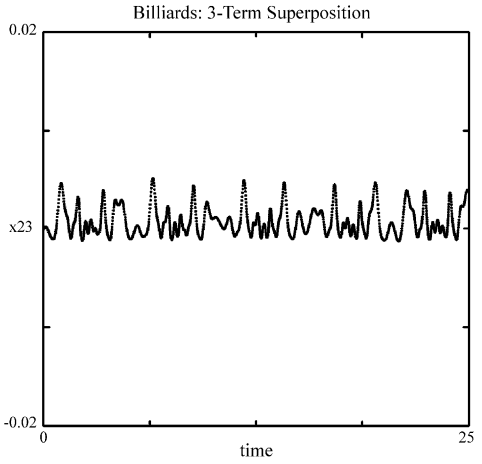

Fig. 15. Time series in $x_{23}(t)$ from $t = 0$ to 25 revealing chaotic behavior.

of the horizontal and vertical motions. In the commensurate case, one obtains periodic motion, whereas in the incommensurate situation, the motion is quasiperiodic [19,48]. In terms of KAM theory, commensurate frequencies correspond to resonant tori (which are destroyed by all perturbations from integrability), and incommensurate ones correspond to nonresonant tori (some of which survive depending on the strength of the perturbation and how poorly the irrational number in question is approximated by a rational number). In the present situation, there are three fundamental interactions, of which two are independent (because the system has two quantum-mechanical dof). In the present context, two eigenstates are said to be "commensurate" when their interaction is regular (up to the precision of our numerical simulations) and "incommensurate" when it is chaotic. In the latter case, the corresponding fundamental coupling mode of the two eigenstates has been excited and clearly displays chaotic features.

In general, when all the frequencies are completely excited, one expects to observe plots without KAM islands (or with very few islands), whereas if one or more of the frequencies is unexcited or partially excited, we observe complicated KAM island structures. (That is, there are regions of both chaotic and integrable behavior.) To phrase the above analysis more rigorously, we remark that a two-term superposition state approximates an infinite dof Hamiltonian system (which describes the full dynamics of the vibrating billiard) with a two dof Hamiltonian system. As discussed previously, a two-term superposition state may be used to describe the nonadiabatic dynamics of twofold electronic near-degeneracies in molecular systems. From a mathematical perspective, one ignores the other dof of the vibrating quantum billiard. Although these dof contribute non-negligibly to the dynamics of the billiard from a mathematical perspective, they are justifiably ignored on physical grounds. Likewise, three-term superposition states yield a *three* dof Hamiltonian system to describe nonadiabatic dynamics in molecular systems near triple electronic near-degeneracies. As a result one may observe more intricate behavior. In particular, this implies that if a single nuclear dof of a molecular system is excited, it must have at least a triple electronic near-degeneracy in order to exhibit Arnold diffusion, cross-resonance diffusion, and other forms of resonant chaos [22,29]. Arnold diffusion has been studied in a two-dimensional Fermi bouncing-ball ("accelerator") model [2,29]. Vibrating quantum billiards are a more general form of the Fermi accelerator model, so one expects to find Arnold diffusion in vibrating quantum billiards with three or more dof. In the context of molecular vibrations, a molecule with one excited nuclear mode, for example, must have at least a triple electronic near-degeneracy in order to exhibit Hamiltonian diffusion. Such behavior may thus have important consequences to nonadiabatic dynamics in polyatomic molecules, nanomechanical devices, and other mesoscopic systems [34,35,46,50].

6. d-Term expansions

We extend our analysis to d-term superposition states. Insert the wavefunction

$$\psi_{(d)}(x,t;a) \equiv \sum_{j=1}^{d} A_{n_j}(t)\psi_{n_j}(x,t;a), \tag{47}$$

which is a superposition of n_1st through n_dth eigenstates into the Schrödinger equation (5). Taking the expectation of both sides of (5) for the state (47) of a one dov quantum billiard yields a generalization of the formulas obtained above (14) and (28):

$$\left\langle \psi_{(d)} \left| -\frac{\hbar^2}{2m}\nabla^2\psi_{(d)} \right\rangle = K(|A_{n_1}|^2,\ldots,|A_{n_d}|^2,a),\right.$$
$$\mathrm{i}\hbar\left\langle \psi \left| \frac{\partial\psi}{\partial t} \right\rangle = \mathrm{i}\hbar\left[\sum_{i,j=1,i\neq j}^{d} \dot{A}_{n_i}A^*_{n_j} + \sum_{i=1}^{d}\nu_{n_in_i}|A_{n_i}|^2 + \sum_{i,j=1,i\neq j}^{d}\nu_{n_in_j}A_{n_i}A^*_{n_j}\right]. \right. \tag{48}$$

Denoting $A_i \equiv A_{n_i}$, the quadratic form (48) leads to the following amplitude equations:

$$\mathrm{i}\dot{A}_k = \sum_{j=1}^{d} D_{kj}A_j. \tag{49}$$

In (49), the diagonal terms of the Hermitian matrix $D \equiv D_{kj}$ are

$$D_{kk} = \frac{\epsilon_{n_k}}{\hbar a^2} \tag{50}$$

and the off-diagonal terms are given by

$$D_{kj} = -\mathrm{i}\mu_{n_kn_j}\frac{\dot{a}}{a}. \tag{51}$$

The parameter $\mu_{kj} \equiv \mu_{n_kn_j} = -\mu_{n_kn_j} \not\equiv 0$ is the coupling coefficient for the cross term $A_{n_k}A^*_{n_j}$. If a coupling coefficient vanishes, the present situation reduces to a lower-dimensional case, so the assumption that none of these coefficients vanishes does not remove any generality.

We transform the complex amplitudes A_j to real variables using a GBT

$$x_{kl} \equiv \rho_{kl} + \rho_{lk}, \qquad y_{kl} \equiv \mathrm{i}(\rho_{lk} - \rho_{kl}), \qquad z_{kl} \equiv \rho_{ll} - \rho_{kk}, \tag{52}$$

where $k < l$. Because $z_{i,i+s} = z_{i,i+1} + \cdots + z_{i+s-1,i+s}$, the GBVs are constrained to parameterize the surface of a (d^2-2)-dimensional ellipsoid:

$$\sum_{i,j=1,i<j}^{d}\left[\frac{d}{2}(x_{ij}^2 + y_{ij}^2) + z_{ij}^2\right] = d-1. \tag{53}$$

As discussed previously, there are additional constraints on the Bloch variables. They are derived with essentially the same calculation as for three-term superposition states, although it is significantly more tedious. With the transformation (52), the kinetic energy may be expressed as

$$K = \frac{2}{da^2}\left[\sum_{k<l} z_{kl}\epsilon^-_{kl} + \epsilon^+\right], \tag{54}$$

where

$$\epsilon_{kl}^{-} \equiv \tfrac{1}{2}(\epsilon_l - \epsilon_k) \tag{55}$$

and

$$\epsilon^{+} \equiv \frac{1}{2}\sum_{j=1}^{d}\epsilon_j. \tag{56}$$

One obtains $(d-1)d/2$ equations of motion for the x-Bloch variables, $(d-1)d/2$ equations of motion for the y-Bloch variables, $(d-1)$ equations for the z-Bloch variables, and Hamilton's equations for $\dot{a}$ and $\dot{P}$. This gives a total of $d^2 - d + d - 1 + 2 = d^2 + 1$ coupled nonlinear ordinary differential equations. The equation for $\dot{x}_{ij}$ takes the form

$$\dot{x}_{ij} = -\frac{\omega_{ij}y_{ij}}{a^2} - \frac{2\mu_{ij}Pz_{ij}}{Ma} + \frac{P}{Ma}\sum_{k=1,k\notin\{i,j\}}^{d} \pm\mu_{ik}x_{kj}, \tag{57}$$

where $\omega_{ij} \equiv (\epsilon_j - \epsilon_i)/\hbar$ as before and the terms in the sum are all negative in the equation for $\dot{x}_{12}$. The terms in the other x-Bloch variable equations are then determined from consistency requirements. More specifically, the Bloch variables are constrained to be on a subset of an ellipsoid. One differentiates the expression describing this constraint (see Appendix A) to obtain the equation

$$\sum_{i,j=1,i<j}^{d}[d(x_{ij}\dot{x}_{ij} + y_{ij}\dot{y}_{ij}) + 2z_{ij}\dot{z}_{ij}] = 0. \tag{58}$$

In order to satisfy (58), the signs of the terms in the sum in Eq. (57) must cancel each other out appropriately. One can thereby determine all the appropriate signs in the equations of motion for the x-Bloch variables from the known signs in the equation for $\dot{x}_{12}$, as the terms in question (that are of the form $x_{ij}x_{kl}$) all come from dynamical equations for other x-Bloch variables.

The equations of motion for the y-Bloch variables take the form

$$\dot{y}_{ij} = \frac{\omega_{ij}x_{ij}}{a^2} + \frac{P}{Ma}\sum_{k=1,k\notin\{i,j\}}^{d} \pm(\mu_{ik}x_{kj} - \mu_{jk}y_{ik}), \tag{59}$$

where all the terms are positive in the dynamical equation for $\dot{y}_{12}$ and the signs of the terms in the other equations are determined using this fact and Eq. (58). The equation for $\dot{z}_{i,i+1}$ takes the form

$$\dot{z}_{i,i+1} = 2\frac{\mu_{i,i+1}Px_{i,i+1}}{Ma} + \frac{P}{Ma}\sum_{k=1,k\notin\{i,i+1\}}^{d}[\mu_{ik}x_{ik} + \mu_{k,i+1}x_{k,i+1}], \tag{60}$$

because all terms with i as the left subscript or $(i+1)$ as the right subscript are necessarily positive. To obtain Eq. (60), we used the fact that $\mu_{nq} = -\mu_{qn}$. Hamilton's equations,

$$\dot{a} = \frac{P}{M} \equiv \frac{\partial H}{\partial P}, \qquad \dot{P} = -\frac{\partial V}{\partial a} - \frac{\partial K}{\partial a} \equiv -\frac{\partial H}{\partial a}, \tag{61}$$

are derived as before using the kinetic and potential energies and the dynamical equations for the z-Bloch variables (60). In particular, one computes that

$$\frac{\partial K}{\partial a} = -\frac{4}{da^3}\left[\sum_{i,j=1,i<j}^{d} z_{ij}\epsilon_{ij}^{-} + \epsilon^{+}\right] + \frac{2}{da^3}\left[\epsilon_{ij}^{-}\left(2\mu_{ij}x_{ij} + \sum_{k=1,k\notin\{i,j\}}^{d}[\mu_{ik}x_{ik} + \mu_{kj}x_{kj}]\right)\right]. \tag{62}$$

The equilibria of the present (d^2+1)-dimensional dynamical system (57) and (59)–(61) satisfy $P=0$, $x_{ij}=y_{ij}=0$, $\sum_{i,j=1,i<j}^{d} z_{ij}^2 = d-1$, and

$$\frac{\partial V}{\partial a} = \frac{4}{da^3}\left[\epsilon^+ + \sum_{i,j=1,i<j}^{d} z_{ij}\epsilon_{ij}^-\right]. \tag{63}$$

The jth equilibrium corresponds to the jth complex amplitude $|A_j|$ having a value of unity and all others vanishing. That is, every equilibrium corresponds to a pure eigenstate with energy

$$E_j = \frac{2\epsilon_j}{a_*^2}, \tag{64}$$

where a_* is the value of the displacement at equilibrium. Each z-Bloch variable must have a value of either 1, 0, or -1 at equilibrium. As a result, the condition (63) may also be expressed as

$$\frac{\partial V}{\partial a}(a_*) = \frac{2\epsilon_j}{a_*^3}, \quad j \in \{1,\ldots,d\}, \tag{65}$$

as shown previously for $d=2,3$. Depending on the form of the external potential $V(a)$, there may be more than one equilibrium corresponding to the jth normal mode. If all the equilibria are elliptic, however, there can only be a single equilibrium corresponding to a given pure state. That is, if one varies a and holds the probability amplitudes constant, the time-derivative of the momentum $\dot{P}$ can vanish precisely once. Thus, since

$$\dot{P} = -\frac{\partial V}{\partial a} - \frac{\partial K}{\partial a}, \tag{66}$$

it follows for d-term superposition states of one dov billiards that if the energy

$$E \equiv V(a) + K(z_{ij}, a) \tag{67}$$

has exactly one minimum with respect to a, then all equilibria are elliptic. In particular, every equilibrium is elliptic for any single-well potential $V(a)$ (including the harmonic potential).

7. Infinite-term expansions

In order to discuss the infinite-term Galërkin expansions that corresponds to the exact dynamics of the system, we treat things in a more abstract context. (We do not consider infinite-term projections in which a finite number of terms are ignored.) A vibrating quantum billiard on an s-dimensional Riemannian manifold (X, g) has wavefunctions defined on the Hilbert space

$$\mathcal{H} = L^2(X \,|\, |x_j| \le 1, \mathrm{d}x) \tag{68}$$

of square-integrable waves ψ with Lebesgue measure $\mathrm{d}x$ [41]. In the above space, the parameter $j \in \{1,\ldots,s\}$ represents the jth coordinate. Although $|x_j| \le a_j(t)$, observe that each coordinate is normalized to unity. The time-dependent boundary components $a_j(t)$ of the billiard appear only as scaling factors in the wavefunction ψ in the Born–Oppenheimer approximation. That is, the wavefunction ψ is expressible as

$$\psi(x_j(t), t; a_j(t)) = \prod_{j=1}^{s} a_j(t)^{\alpha_j}\psi\left(\frac{x_j}{a_j(t)}, t\right) \in \mathcal{H}, \tag{69}$$

where α_j is the power of a_j needed for normalization. In Eq. (69), the variable displacements appear as constant normalization factors in front of the molecular wavefunction ψ and as scalings of the relevant displacement variable.

One may therefore incorporate this scaling in the definition of the Hilbert space $\mathcal{H}$ in which the wavefunction resides. A single normal mode ψ_n has the normalization factor

$$c_j \prod_{j=1}^{s} a_j(t)^{\alpha_j}, \tag{70}$$

where c_j are constants that may be different for each normal mode. On the other hand, the a_j-dependence in the normalization factor is the same for each eigenfunction.

Using this geometric description, we see that vibrating quantum billiards have an infinite-dimensional Hamiltonian structure with Hamiltonian given by the energy

$$E[\psi, a, \dot{a}] = \int_{\{|x_j| \le a_j\}} \|\nabla\psi\|^2 \, \mathrm{d}x + \sum_{j=1}^{s} \frac{M_j}{2}\dot{a}_j^2 + V(a_1, \ldots, a_s). \tag{71}$$

Using $\dot{a}_j = P_j/M_j$, we obtain s equations describing the mechanical motion of the billiard boundary:

$$M_j\ddot{a}_j = \dot{P}_j = -\int_{\{|x_j| = a_j\}} \|\nabla\psi\|^2 \, \mathrm{d}\sigma(x) - \frac{\partial V}{\partial a_j}, \tag{72}$$

where $\mathrm{d}\sigma(x)$ is a Lebesgue measure on the boundary of the billiard. Finally, note that this formulation is for s dov vibrating quantum billiards.

Now that we have discussed the Hilbert space setting of the present system, let us consider the Lie group structure of the associated wavefunction ψ. Since the wave is normalized, we immediately restrict ourselves to the unitary group on $\mathbb{C}^d$, where d is the number of terms in the superposition state. Because of their scale-invariance—two wavefunctions are equivalent if one is a multiple of the other—wavefunctions may be treated as elements of the complex projective space $\mathbb{CP}^{d-1}$, which is the set of lines in $\mathbb{C}^d$, or equivalently the set $\mathbb{C}^d/\{\text{change of scales}\}$. If one is not taking a Galërkin truncation, then $d = \infty$ and one has a basis of infinitely many normal modes with coefficients $A_i \in \mathbb{C}$. In this case, we are dealing with the group $\mathbb{C}^\infty$ and hence $\mathbb{CP}^\infty$. The infinite-dimensional projective space $\mathbb{CP}^\infty$ is given by the union

$$\mathbb{CP}^\infty = \bigcup_{j \ge 0} \mathbb{CP}^j. \tag{73}$$

It is well-defined because of the embedding $\mathbb{CP}^j \hookrightarrow \mathbb{CP}^{j+1}$, which is defined by appending a 0 to the last coordinate of any point $\zeta^j \in \mathbb{CP}^j$.

By conservation of probability, the sum of the squared amplitudes $|A_j|^2$ is unity. This entails restrictions on the density matrix $\rho_{jk} = A_j A_k^*$, which we may write as a projection operator

$$\rho \equiv P_\varphi, \tag{74}$$

where $P_\varphi\psi = \langle\psi, \varphi\rangle\varphi$ for the $\{\varphi\}$-basis. For a given basis $\{\psi_j\}$, a wave function is determined by its amplitude tuple $\{A_j\} \equiv \{A_{m_1}, \ldots, A_{m_j}, \ldots\}$. Conservation of probability, $\sum_{j=1}^{d} |A_j|^2 = 1$, follows from the fact that $\psi \in \mathrm{U}(\mathbb{C}^d)$. Furthermore, as the global phase of wave-function ψ is unimportant, ψ is actually an element of the quotient group

$$\frac{\mathrm{U}(\mathbb{C}^d)}{\{\mathrm{e}^{\mathrm{i}\theta} I\}}, \tag{75}$$

where $\{\mathrm{e}^{\mathrm{i}\theta} I\}$, the set of all global phase shifts, is the center of the group $\mathrm{U}(\mathbb{C}^d)$. (Recall that the center of a group is the subgroup whose elements commute with every element of the group [17]. In a quantum-mechanical setting, this corresponds to the set of all global phase factors.) If d is finite, then $\psi \in \mathrm{U}(d)/\{\mathrm{e}^{\mathrm{i}\theta} I\}$. There is thus a natural

action of the group $\mathrm{U}(d)/\{\mathrm{e}^{\mathrm{i}\theta} I\} : \mathbb{C}^d \to \mathbb{C}^d$ which induces an action from $\mathbb{CP}^{d-1}$ to $\mathbb{CP}^{d-1}$ by the invariance of wavefunctions under scaling. The group $\mathrm{U}(d)/\{\mathrm{e}^{\mathrm{i}\theta} I\}$ is the invariance group of the action described above. In the infinite-term case, one similarly has an action

$$\frac{\mathrm{U}(\mathbb{C}^d)}{\{\mathrm{e}^{\mathrm{i}\theta} I\}} : \mathbb{CP}^{\infty} \to \mathbb{CP}^{\infty} \tag{76}$$

under the invariance group $\mathrm{U}(\mathbb{C}^d)/\{\mathrm{e}^{\mathrm{i}\theta} I\}$.

In the present abstract setting, one defines ψ to be an element of its invariant Lie group, as on the normalized Hilbert space $\mathcal{H}$ (in which the time-dependence of $a(t)$ makes no difference), it is completely determined by its coefficients A_j (and hence by its associated Bloch variables):

$$\psi = \sum_j A_j \psi_j . \tag{77}$$

This leads to another way for determining well-posedness of vibrating quantum billiards. One can do this with Hilbert spaces (as we did above), or one can simply proceed by hand. Using the latter perspective, the vibrating quantum billiard problem is well-posed by choosing a basis of eigenfunctions $\{\psi_j\}$ accompanied by initial complex amplitudes $A_j(0)$.

In the action of the invariant group, one generally has an $\infty : 1$ map. However, if one restricts one's attention to the *finite-dimensional* subgroup $\mathrm{U}(d)/\{\mathrm{e}^{\mathrm{i}\theta} I\} \subset \mathrm{U}(\mathbb{C}^{\infty})/\{\mathrm{e}^{\mathrm{i}\theta} I\}$, one instead obtains a $d : 1$ map. This procedure is equivalent to taking a d-term Galërkin projection. In general, for $d \geq n$ (including $d = \infty$), one obtains an $n : 1$ map by restricting the wave-function $\psi \in \mathrm{U}(n)/\{\mathrm{e}^{\mathrm{i}\theta} I\}$.) In other words, the act of taking a d-term Galërkin projection corresponds to restricting the Lie group in which the wave-function resides. (The fact that the map is $d : 1$ implies, for instance, that one takes d roots of unity in the inverse map.) This, in turn, is accomplished by restricting the coefficient tuple $\{A_j\}$ to be an element of $\mathbb{C}^d$ (and retaining the invariance properties of the coefficients that are consequences of the invariance properties of ψ).

By considering d-term superposition states, we thus see that the Lie algebra $\mathfrak{u}(\mathfrak{d})/\{\mathfrak{e}^{\mathrm{i}\theta}\, \mathfrak{I}\}$ of the Lie group $\mathrm{U}(d)/\{\mathrm{e}^{\mathrm{i}\theta} I\}$ is isomorphic to the Lie algebra $\mathfrak{su}(\mathfrak{d})$ of $\mathfrak{su}(\mathfrak{d})$. However, their associated Lie groups are not themselves isomorphic. When d is odd, for example, $\mathrm{U}(d)/\{\mathrm{e}^{\mathrm{i}\theta} I\}$ has a trivial center, whereas $-I$ is in the center of $\mathrm{SU}(d)$. Moreover, when $d = 2$, the group $\mathrm{U}(2)/\{\mathrm{e}^{\mathrm{i}\theta} I\}$ is isomorphic to the rotation group $\mathrm{SO}(3)$, which is not isomorphic to $\mathrm{SU}(2)$, as the latter group is simply connected and the former is not. Nevertheless, because their Lie algebras are isomorphic, there necessarily exists a map from the neighborhood of the identity of one group onto a neighborhood of the identity of the other group which is a homomorphism where it is defined. In other words, $\mathrm{U}(d)/\{\mathrm{e}^{\mathrm{i}\theta} I\}$ and $\mathrm{SU}(d)$ are "locally isomorphic" [15].

As briefly mentioned above, the analysis in the present section shows that the vibrating quantum billiard problem is well-posed whether or not one approximates the system with a finite-term superposition (Galërkin projection). This follows from the well-definedness of the Hilbert space structure. We note that we did not need to form a basis of eigenstates in order to demonstrate this. Nevertheless, the well-posedness of the present problem may also be demonstrated using such an explicit basis.

In addition to discussing the symmetries of vibrating quantum billiards, one may utilize infinite-term Galërkin expansions to write such systems as infinite sets of coupled nonlinear ordinary differential equations. The dynamical equations for the complex amplitudes are given by

$$\mathrm{i}\dot{A}_k = \sum_{j=1}^{\infty} D_{kj} A_j , \tag{78}$$

where the matrix elements D_{kj} are defined as before. Although the dynamics of the quantum dof of vibrating quantum billiards can be written using Eq. (78), it is not convenient to analyze these systems in this manner. Using an action–angle formulation would simplify the resulting equations, but for now we stop at the present geometric treatment. With such analysis, the techniques of geometric mechanics [31] may eventually prove quite fruitful for vibrating quantum billiards and related molecular systems.

8. d-Term expansions in quantum billiards with two or more dov

The ideas discussed in the present paper may also be applied to quantum billiards with more than one dov. Recall that the dov of a quantum billiard refer to the classical dof describing the dynamics of the billiard boundary. Thus, a two-mode Galërkin expansion of a two dov quantum billiard has three total dof (as there is also one quantal dof). Such a configuration could therefore exhibit Hamiltonian diffusion. An important difference between such systems and those discussed previously are the relative numbers of fast and slow dof. That is, a two-term superposition state of a two dov quantum billiard is very different from a three-term superposition state of a one dov quantum billiard, even though both problems are three dof Hamiltonian systems. The former system has two slow dof and one fast one, whereas the latter one has one fast dof and two slow ones.

9. Conclusions

We considered superposition states of various numbers of terms in order to analyze vibrating quantum billiards from a semiquantum perspective. We discussed the relationship between Galërkin methods, inertial manifolds, and other differential equations such as NLS equations. We then studied vibrating quantum billiards by considering one-term, two-term, three-term, d-term, and infinite-term superposition states. We derived a GBT that is valid for any finite-term superposition and numerically simulated three-mode Galërkin expansions of the radially vibrating spherical quantum billiard with null angular-momentum eigenstates. We discussed the physical interpretation of d-term superposition states in terms of d-fold electronic near-degeneracies and thereby justified the use of a Galërkin approach to the study of vibrating quantum billiards. Finally, we applied geometric methods to analyze the symmetries of infinite-term superpositions.

Acknowledgements

We gratefully acknowledge Greg Ezra, Len Gross, Jerry Marsden and Paolo Zanardi for useful discussions concerning this project. Additionally, we thank the referees for several useful suggestions that improved this paper immensely.

Appendix A. Semiquantum chaos

Semiquantum chaos refers to chaos in systems with both classical and quantum components [9]. Although typically studied in the context of conservative systems (so that one is considering Hamiltonian chaos in the semiquantum regime), semiquantum chaos can occur in dissipative systems as well [16,35,37].

Semiquantum descriptions typically arise from the dynamic Born–Oppenheimer approximation, which is applied constantly in molecular physics [4,7,8,35,46]. Part of the value of semiquantum physics is that one may observe chaos

even in low-energy systems, such as nuclei that have been coupled to two-level electronic systems consisting of the ground state and the first excited state of appropriate symmetry [28,35,39]. In the setting of quantum chaology (i.e., quantized chaos), which is the type of quantum chaos ordinarily considered, one typically focuses on highly energetic states [9,20,21]. Thus, the semiquantum regime is important for capturing the chaotic dynamics of low-energy states. As this phenomenon has been observed experimentally in molecular systems [46], semiquantum chaos is an important type of quantum chaotic behavior.

Both the classical and quantal components of semiquantum systems can behave chaotically. Chaos in the quantum subsystem manifests in the quantum probabilities. Even the chaotic dynamics of the classical subsystem has quantum consequences, however, as the quantum normal modes and eigenenergies of a semiquantum system depend on its classical dof. Hence, the wavefunctions of semiquantum chaotic systems exhibit quantum-mechanical *wave chaos* [8,39]. Additionally, as the lengthscales of the wavefunctions are determined by the classical dof, semiquantum chaos leads to a chaotic superposition of chaotic normal modes.

To consider the wavefunction lengthscales of vibrating quantum billiards in more detail, note that the displacement $a(t)$ considered in this work represents a characteristic length of the eigenstates because the argument of each of the normal modes of one dov quantum billiards (before normalization) is proportional to a^{-1}. For example, the one-dimensional vibrating quantum billiard [8,9] contains modes of the following form:

$$\cos\left(\frac{k\pi x}{a}\right), \qquad \sin\left(\frac{k\pi x}{a}\right). \tag{A.1}$$

The inverse displacement $a(t)^{-1}$ thus plays the role of a wavenumber and $a(t)$ plays the role of a wavelength. Consequently, chaotic behavior in $a(t)$ represents chaotic evolution in normal mode wavelengths. The momentum $P(t)$ measures the change in the wavefunction's lengthscale, as the dynamics of the wavelengths of each of the eigenfunctions are described by the motion of a. (Each of these wavelengths is a constant multiple of $a(t)$.) This interpretation also holds for multiple dov quantum billiards—there is a characteristic lengthscale corresponding to each dov.

The signature of semiquantum chaos in real space is the sequence of intersections with a fixed displacement that nodal surfaces make at any instant subsequent to a number of transversal times [28]. At $t = t_1$, the normal modes $\psi_j \equiv \psi_j(x, y, z, t; a(t))$ each vanish for a countably infinite set of values of (x, y, z) (which are determined by $a(t_1)$). At $t = t_2 > t_1$, ψ_j vanishes for another countably infinite set of values of (x, y, z), etc. (The notation ψ_j is used to denote the jth eigenfunction in a d-mode Galërkin expansion.) The number of transversal times in the sequence $\{t_1, \ldots, t_k\}$ refers to the number k, which describes how many times the system of interest has been strobed (i.e., the number of dots in a Poincaré section).

In the language of Blümel and Reinhardt [9] as well as our previous work [28,38–40], vibrating quantum billiards can exhibit semiquantum chaos. One has a classical system (the walls of the billiard) coupled to a quantum-mechanical one (the particle enclosed by the billiard boundary). Considered individually, each of these subsystems is integrable provided there is a single classical dof. When a vibrating billiard's classical and quantum components interact, however, one observes chaotic behavior in each of them. Note finally that quantizing the motion of the billiard walls leads to a higher-dimensional, fully quantized system that exhibits so-called quantized chaos [9].

Appendix B. Generalized Bloch representations

In this appendix, we derive a canonical "generalized Bloch representation" (GBR) corresponding to d-term superpositions [15,49]. We begin with a discussion of the geometry underlying this representation, which yields a

"generalized Bloch sphere" (GBS). We then discuss the cases $d = 2$ and 3 and briefly generalize the analysis to higher-term superposition states. For $d = 2$, we utilize the standard Bloch sphere, whereas for $d = 3$, we make a transformation by hand to obtain variables that are more convenient for our analysis than the canonical GBR.

The appropriate function space of a d-term Galërkin projection is a d-dimensional Hilbert space $\mathcal{H}$. The group End($\mathcal{H}$) of linear operators ("endomorphisms") over $\mathcal{H}$ is metrizeable in several manners [17]. In the present context, we use the metric

$$d(A, B) = \sqrt{\tfrac{1}{2}\langle A - B, A^\dagger - B^\dagger\rangle} \tag{B.1}$$

induced by the Hilbert–Schmidt inner product $\langle A, B\rangle$. The Lie algebra of Hermitian $d \times d$ traceless matrices $\mathfrak{su}(\mathfrak{d})$ is a D-dimensional ($D = d^2 - 1$) real subspace of End($\mathcal{H}$) [15]. We choose a basis $\{\tau_j\}_{j=1}^{D}$ of $\mathfrak{su}(\mathfrak{d})$ so that $\langle \tau_j, \tau_k\rangle = 2\delta_{jk}$. The set $\mathcal{B}_1$ of Hermitian operators with unit trace is a D-dimensional hyperplane of End($\mathcal{H}$). Any element $\rho \in \mathcal{B}_1$ may be written in the form

$$\rho(\lambda) = \frac{1}{d} I + \frac{1}{2}\sum_{j=1}^{D} \lambda_j \tau_j, \tag{B.2}$$

where the vector $\lambda \equiv (\lambda_1, \ldots, \lambda_D) \in \mathbb{R}^D$ is the GBR of ρ. Eq. (B.2) defines a map $m : \mathcal{B}_1 \to \mathbb{R}^D$ that associates with any ρ its GBR vector, so $\rho \equiv \rho[m(\rho)]$ [49].

Suppose $\mathbb{R}^D$ is endowed with the canonical Euclidean inner product. Let $S^{D-1} \subset \mathbb{R}^D$ be the $(D-1)$-dimensional hypersphere with radius

$$R_d = \sqrt{2\left(1 - \frac{1}{d}\right)}, \tag{B.3}$$

and let B_D be the ball bounded by S^{D-1}. If $d = 2$, one finds that $R_2 = 1$, which recovers the Bloch sphere S^2. In the context of the present paper, one transforms the complex amplitudes A_1 and A_2 to (real) Bloch variables via the transformation

$$x \equiv \rho_{12} + \rho_{21}, \tag{B.4}$$

$$y \equiv \mathrm{i}(\rho_{21} - \rho_{12}), \tag{B.5}$$

$$z \equiv \rho_{22} - \rho_{11}, \tag{B.6}$$

where $\rho_{qn} = A_q A_n^*$ is the density matrix [27]. Because $|A_1|^2 + |A_2|^2 = 1$, it follows that $x^2 + y^2 + z^2 = 1$.

For $d \geq 3$, it is more convenient for our purpose to use a slightly different transformation. We therefore generalize the explicit form of the two-dimensional Bloch transformation rather than the geometric aspect highlighted above. We construct these transformations for $d = 3$ and 4. One should note several facts regarding GBRs. The radii of "Bloch ellipsoids" (which are described by one of our constraints) depend on the normalization of the D generators of $\mathfrak{su}(\mathfrak{d})$. The geometric description above reduces to the standard representation for $d = 2$ (Pauli spin matrices) and $d = 3$ (Gell–Mann matrices).

A generic Hermitian matrix is described by d^2 independent parameters. In the present case, however, the constraint

$$\mathrm{tr}(\rho) = \sum_{j=1}^{d} |A_j|^2 = 1 \tag{B.7}$$

coupled with the fact that the physical manifestation of wavefunctions is invariant under changes in the *absolute phase* of the system reduces the number of Bloch variables by 2 to $(d^2 - 2)$. (The second statement says that one can

shift *every* normal mode by the same phase without altering the physics. However, the relative phases of the normal modes are very important. The operation of ignoring the system's absolute phase corresponds mathematically to modding out by the group $\{e^{i\vartheta} I\}$, where ϑ is an arbitrary phase.) This number of Bloch variables does not correspond to the number of quantum dof of the present system, which is $d-1$. (In a d-term Galërkin projection, one has d complex amplitudes and hence $2d$ real variables. Because of the normalization constraint and invariance under global phase shifts, one obtains $(2d-2)$ independent real variables and hence $(d-1)$ quantal dof.) Consequently, the nine Bloch variables for three-term superpositions are accompanied by five constraints, and the 18 Bloch variables for four-term superpositions require 10 constraints. Thus, this naive construction becomes cumbersome rather quickly. Nevertheless, it can be insightful to derive it for small values of d.

When $d=3$, there are three complex amplitudes A_1, A_2 and A_3. For $k<l$, define

$$x_{kl} \equiv \rho_{kl} + \rho_{lk}, \qquad y_{kl} \equiv \mathrm{i}(\rho_{lk} - \rho_{kl}), \qquad z_{kl} \equiv \rho_{ll} - \rho_{kk}. \tag{B.8}$$

The transformations (B.8) yields nine variables, so there must be two associated constants of motion, since we seek to describe a seven-"ellipsoid". (There are then three additional constants of motion, so one is actually considering subsets of this ellipsoid.) It is apparent that $z_{13} = z_{12} + z_{23}$, and one can compute that

$$\sum_{k<l} [\tfrac{3}{2}(x_{kl}^2 + y_{kl}^2) + z_{kl}^2] = 2(|A_1|^2 + |A_2|^2 + |A_3|^2) = 2 \cdot 1 = 2. \tag{B.9}$$

Defining $z_1 \equiv z_{12}$ and $z_2 \equiv z_{23}$ yields a Bloch seven-ellipsoid with eight generators $\{x_{12}, x_{13}, x_{23}, y_{12}, y_{13}, y_{23}, z_1, z_2\}$ and the constraint

$$\frac{3}{2}\left(\sum_{k<l} x_{kl}^2 + \sum_{k<l} y_{kl}^2\right) + 2(z_1^2 + z_1 z_2 + z_2^2) = 2. \tag{B.10}$$

We now derive the other constraints. From the standard Bloch variable construction [1], observe that

$$\begin{aligned} &x_{12}^2 + y_{12}^2 + z_{12}^2 = [1 - |A_3|^2]^2, \qquad x_{13}^2 + y_{13}^2 + z_{13}^2 = [1 - |A_2|^2]^2, \\ &x_{23}^2 + y_{23}^2 + z_{23}^2 = [1 - |A_1|^2]^2. \end{aligned} \tag{B.11}$$

Taking the square root of Eqs. (B.11) produces two constraints:

$$\begin{aligned} z_{12} &= \sqrt{x_{23}^2 + y_{23}^2 + z_{23}^2} - \sqrt{x_{13}^2 + y_{13}^2 + (z_{12} + z_{23})^2}, \\ z_{23} &= \sqrt{x_{13}^2 + y_{13}^2 + (z_{12} + z_{23})^2} - \sqrt{x_{12}^2 + y_{12}^2 + z_{12}^2}. \end{aligned} \tag{B.12}$$

We obtain a final constraint by summing the three equations (B.11):

$$2 = \sum_{k<l}^{3} \sqrt{x_{kl}^2 + y_{kl}^2 + z_{kl}^2}. \tag{B.13}$$

Let us briefly consider the case of general d. For $k<l$, define

$$x_{kl} \equiv \rho_{kl} + \rho_{lk}, \qquad y_{kl} \equiv \mathrm{i}(\rho_{lk} - \rho_{kl}), \qquad z_{kl} \equiv \rho_{ll} - \rho_{kk}, \tag{B.14}$$

as before. This yields $3d!/[2 \cdot (d-2)!]$ variables, which needs to be reduced to (d^2-1) variables. We also need to find several constraints for the reduced set of variables in order to obtain $[2(d-1)]$ independent variables

(corresponding the system's $(d-1)$ dof). To find the constraint associated with the Bloch ellipsoid, one needs to find constants α and β such that

$$\sum_{i,j=1,i<j}^{d} [\alpha(x_{ij}^2 + y_{ij}^2) + z_{ij}^2] = \beta. \tag{B.15}$$

The above equation is satisfied if and only if $\alpha = d/2$ and $\beta = d-1$. For $d = 2$, one obtains the constraint $x^2 + y^2 + z^2 = 1$. The case $d = 3$ also reproduces our previous result. For $d = 4$, we find that $\alpha = 2$ and $\beta = 3$. The relative contributions of x_{ij} and y_{ij} increase faster than those of z_{ij}, so using this explicit GBR generates ellipsoids rather than spheres for $d > 2$. The constraints for $d = 3$ are tractable, but things become ridiculously messy for $d = 4$. We illustrate this construction in the present paper, but we restrict our numerical simulations to $d \leq 3$.

One reduces the number of variables by considering only z_{ij} such that $j - i = 1$. Thus, for $d = 4$, we use the variables z_{12}, z_{23}, and z_{34} to obtain 15 Bloch variables with a normalization constraint that gives us a 14-ellipsoid. It follows from Eq. (B.8) that

$$z_{ik} \equiv \rho_{kk} - \rho_{ii} = (\rho_{kk} - \rho_{jj}) + (\rho_{jj} - \rho_{ii}) \equiv z_{ij} + z_{jk}. \tag{B.16}$$

Applying (B.16) recursively then implies that

$$z_{i,i+s} = z_{i,i+1} + \cdots + z_{i+s-1,i+s}. \tag{B.17}$$

For example, $z_{14} = z_{12} + z_{23} + z_{34}$. The other six constraints for the $d = 4$ case are derived from the six equations

$$x_{ij}^2 + y_{ij}^2 + z_{ij}^2 = [1 - |A_k|^2 - |A_l|^2]^2, \tag{B.18}$$

where i, j, k, and l are distinct indices in $\{1, 2, 3, 4\}$. Three of these equations take the form

$$\sqrt{x_{ij}^2 + y_{ij}^2 + z_{ij}^2} + \sqrt{x_{kl}^2 + y_{kl}^2 + z_{kl}^2} = 1, \tag{B.19}$$

where all the indices are again distinct. (One then inserts the appropriate relations between the z-Bloch variables.) The other three equations are

$$\begin{aligned}
-\sqrt{x_{12}^2 + y_{12}^2 + z_{12}^2} + \sqrt{x_{34}^2 + y_{34}^2 + z_{34}^2} &= z_{14} + z_{23} = z_{12} + 2z_{23} + z_{34}, \\
-\sqrt{x_{13}^2 + y_{13}^2 + z_{13}^2} + \sqrt{x_{24}^2 + y_{24}^2 + z_{24}^2} &= z_{12} + z_{34}, \\
-\sqrt{x_{14}^2 + y_{14}^2 + z_{14}^2} + \sqrt{x_{23}^2 + y_{23}^2 + z_{23}^2} &= z_{12} - z_{34},
\end{aligned} \tag{B.20}$$

where we have utilized the previously derived conditions for the z-Bloch variables. This analysis, then, gives a prescription for explicit GBVs to complement the equivalent Lie group formulation presented earlier (for which the number of dof of the system was not directly evident).

A different transformation to obtain real variables related to the complex amplitudes A_k is to use action–angle coordinates [35,46]. In this construction, one defines the kth action n_k and kth angle θ_k with the relation

$$A_k \equiv \sqrt{n_k}\, \mathrm{e}^{\mathrm{i}k\theta}. \tag{B.21}$$

This produces $d-1$ dof because of conservation of probability and invariance of wavefunctions under global phase shifts. In this new notation, conservation of probability implies that the actions satisfy the condition

$$\sum_{k=1}^{d} n_k = 1. \tag{B.22}$$

Analysis of vibrating quantum billiards in this action–angle formulation should be a fruitful endeavor. This formulation, in fact, arises frequently in the chemical physics literature, so there is precedent for this perspective [32,46,50]. Action–angle coordinates have the advantage that the number of quantum dof become more transparent. On the other hand, the GBR has the advantage that the geometric structure of vibrating quantum billiards (and Galërkin truncations thereof) is more easily seen. (Moreover, the use of Bloch variables circumvents the need for the so-called "Langer modification" [23].) Although we take the latter approach in the present paper, we note that an action–angle approach will allow more analytical discussions of semiquantum chaos and diffusion. This will thus be the subject of future work.

References

[1] L. Allen, J.H. Eberly, Optical Resonance and Two-level Atoms, Dover, New York, 1987.
[2] R. Badrinarayanan, J.V. José, Spectral properties of a Fermi accelerating disk, Physica D 83 (1995) 1–29.
[3] A. Barelli, J. Bellissard, P. Jacquod, D.L. Shepelyanksy, Two interacting Hofstadter butterflies, Phys. Rev. B 55 (15) (1997) 9524–9533.
[4] G. Baym, Lectures on Quantum Mechanics, Lecture Notes and Supplements in Physics, Perseus Books, Reading, MA, 1990.
[5] C.M. Bender, S.A. Orszag, Advanced Mathematical Methods for Scientists and Engineers, McGraw-Hill, New York, 1978.
[6] I.B. Bersuker, Modern aspects of the Jahn–Teller effect theory and applications to molecular problems, Chem. Rev. 101 (2001) 1067–1114.
[7] I.B. Bersuker, V.Z. Polinger, Vibronic Interactions in Molecules and Crystals, Vol. 49 in Springer Series in Chemical Physics, Springer, New York, 1989.
[8] R. Blümel, B. Esser, Quantum chaos in the Born–Oppenheimer approximation, Phys. Rev. Lett. 72 (23) (1994) 3658–3661.
[9] R. Blümel, W.P. Reinhardt, Chaos in Atomic Physics, Cambridge University Press, Cambridge, UK, 1997.
[10] F. Borgonovi, D.L. Shepelyansky, Particle propagation in a random and quasi-periodic potential, Physica D 109 (1997) 24–31.
[11] G. Casati, B. Chirikov, Quantum Chaos, Cambridge University Press, New York, 1995.
[12] G. Casati, I. Guarneri, D.L. Shepelyanksy, Anderson transition in a one-dimensional system with three incommensurate frequencies, Phys. Rev. Lett. 62 (4) (1989) 345–348.
[13] G. Casati (Ed.), Chaotic Behavior in Quantum Systems, Plenum Press, New York, 1985.
[14] D.F. Coker, L. Xiao, Methods for molecular dynamics with nonadiabatic transitions, J. Chem. Phys. 102 (1) (1995) 496–510.
[15] J.F. Cornwell, Group Theory in Physics, Vol. 2, Harcourt, Brace and Jovanovich, London, UK, 1984.
[16] J. Diggins, J.F. Ralph, T.P. Spiller, T.D. Clark, H. Prance, R.J. Prance, Chaotic dynamics in the rf superconducting quantum-interference-device magnetometer: a coupled quantum-classical system, Phys. Rev. E 49 (3) (1994) 1854–1859.
[17] D.S. Dummit, R.M. Foote, Abstract Algebra, Prentice-Hall, Englewood Cliffs, NJ, 1991.
[18] A. Friedman, Free boundary problems in science and technology, Notices Am. Math. Soc. 47 (8) (2000) 854–861.
[19] J. Guckenheimer, P. Holmes, Nonlinear Oscillations, Dynamical Systems, and Bifurcations of Vector Fields, Vol. 42 in Applied Mathematical Sciences, Springer, New York, 1983.
[20] M.C. Gutzwiller, Chaos in Classical and Quantum Mechanics, Vol. 1 in Interdisciplinary Applied Mathematics, Springer, New York, 1990.
[21] F. Haake, Quantum Signatures of Chaos, 2nd Edition, Springer Series in Synergetics, Springer, Berlin, 2001.
[22] G. Haller, Chaos Near Resonance, Vol. 138 in Applied Mathematical Sciences, Springer, New York, 1999.
[23] M.F. Herman, R. Currier, A justification for the use of the Langer modification in Miller's classic analog method of non-adiabatic scattering, Chem. Phys. Lett. 114 (4) (1985) 411–414.
[24] G. Herzberg, H.C. Longuet-Higgins, Intersection of potential energy surfaces in polyatomic molecules, Discuss. Faraday Soc. 35 (1963) 77–82.
[25] M.H. Holmes, Introduction to Perturbation Methods, Vol. 20 in Texts in Applied Mathematics, Springer, New York, 1995.
[26] C. Johnson, Numerical Solution of Partial Differential Equations by the Finite Element Method, Cambridge University Press, Cambridge, UK, 1987.
[27] R.L. Liboff, Introductory Quantum Mechanics, 3rd Edition, Addison-Wesley, San Francisco, CA, 1998.
[28] R.L. Liboff, M.A. Porter, Quantum chaos for the radially vibrating spherical billiard, Chaos 10 (2) (2000) 366–370.
[29] A.J. Lichtenberg, M.A. Lieberman, Regular and Chaotic Dynamics, 2nd Edition, Vol. 38 in Applied Mathematical Sciences, Springer, New York, 1992.
[30] R.S. Markiewicz, Chaos in a Jahn–Teller molecule, Phys. Rev. E 64 (026216) (2001) 1–5.
[31] J.E. Marsden, T.S. Ratiu, Introduction to Mechanics and Symmetry, 2nd Edition, Vol. 17 in Texts in Applied Mathematics, Springer, New York, 1999.
[32] H.-D. Meyer, W.H. Miller, A classical analog for electronic degrees of freedom in nonadiabatic collision processes, J. Chem. Phys. 70 (7) (1979) 3214–3223.
[33] B. Mirbach, G. Casati, Transition from quantum ergodicity to adiabaticity: dynamical localization in an amplitude modulated pendulum, Phys. Rev. Lett. 83 (7) (1999) 1327–1330.

[34] H. Park, J. Park, A.K. Lim, E.H. Anderson, A.P. Alivisatos, P.L. McEuen, Nanomechanical oscillations in a single C_{60} transistor, Nature 407 (2000) 57–60.
[35] M.A. Porter, Nonadiabatic dynamics in semiquantal physics, Rep. Prog. Phys. 64 (9) (2001) 1165–1190.
[36] M.A. Porter, R.L. Liboff, Bifurcations in one degree-of-vibration quantum billiards, Int. J. Bifurc. Chaos 11 (4) (2001) 903–911.
[37] M.A. Porter, R.L. Liboff, Chaos on the quantum scale, Am. Sci. 89 (6) (2001) 532–537.
[38] M.A. Porter, R.L. Liboff, Quantum chaos for the vibrating rectangular billiard, Int. J. Bifurc. Chaos 11 (9) (2001) 2317–2337.
[39] M.A. Porter, R.L. Liboff, The radially vibrating spherical quantum billiard, Discrete and Continuous Dynamical Systems, 2001, pp. 310–318, in: Proceedings of the Third International Conference on Dynamical Systems and Differential Equations, Kennesaw State University, Georgia, May 2000.
[40] M.A. Porter, R.L. Liboff, Vibrating quantum billiards on Riemannian manifolds, Int. J. Bifurc. Chaos 11 (9) (2001) 2305–2315.
[41] W. Rudin, Real and Complex Analysis, 3rd Edition, McGraw-Hill, New York, 1987.
[42] D.L. Shepelyanksy, A.D. Stone, Chaotic Landau level mixing in classical and quantum wells, Phys. Rev. Lett. 74 (11) (1995) 2098–2101.
[43] B. Space, D.F. Coker, Nonadiabatic dynamics of excited excess electrons in simple fluids, J. Chem. Phys. 94 (3) (1991) 1976–1984.
[44] B. Space, D.F. Coker, Dynamics of trapping and localization of excess electrons in simple fluids, J. Chem. Phys. 96 (1) (1992) 652–663.
[45] R. Temam, Infinite-dimensional Dynamical Systems in Mechanics and Physics, 2nd Edition, Vol. 68 in Applied Mathematical Sciences, Springer, New York, 1997.
[46] R.L. Whetten, G.S. Ezra, E.R. Grant, Molecular dynamics beyond the adiabatic approximation: new experiments and theory, Annu. Rev. Phys. Chem. 36 (1985) 277–320.
[47] G.B. Whitham, Linear and Nonlinear Waves, Pure and Applied Mathematics, Wiley/Interscience, New York, 1974.
[48] S. Wiggins, Introduction to Applied Nonlinear Dynamical Systems and Chaos, Vol. 2 in Texts in Applied Mathematics, Springer, New York, 1990.
[49] P. Zanardi, Quantum cloning in d dimensions, Phys. Rev. A 58 (5) (1998) 3484–3490.
[50] J.W. Zwanziger, E.R. Grant, G.S. Ezra, Semiclassical quantization of a classical analog for the Jahn–Teller $E \times e$ system, J. Chem. Phys. 85 (4) (1986) 2089–2098.